MIT

USE AND CHARACTERIZATION OF STEADY-STATE SOIL MOISTURE PROFILE IN SETTING FLUX CAPACITIES PRIOR TO STORM AND INTERSTORM EVENTS

by
GUIDO D. SALVUCCI
and
DARA ENTEKHABI

RALPH M. PARSONS LABORATORY
HYDROLOGY AND WATER RESOURCE SYSTEMS

DEPARTMENT
OF
CIVIL
ENGINEERING

SCHOOL OF ENGINEERING
MASSACHUSETTS INSTITUTE OF TECHNOLOGY
Cambridge, Massachusetts 02139

Report Number 338

Prepared under the support of the National Aeronautics and Space Administration Subcontract No. NAS 5-31721 and Grant No. NAGW 1696

May, 1993

R93-11

USE AND CHARACTERIZATION OF STEADY-STATE SOIL MOISTURE PROFILE IN SETTING FLUX CAPACITIES PRIOR TO STORM AND INTERSTORM EVENTS

by
GUIDO D. SALVUCCI
and
DARA ENTEKHABI

RALPH M. PARSONS LABORATORY
HYDROLOGY AND WATER RESOURCE SYSTEMS

Report Number 338

Prepared under the support of the National Aeronautics and Space Administration
Subcontract No. NAS 5-31721 and Grant No. NAGW 1696

May, 1993

Table of Contents

Table of Contents, continued

Executive Summary

Characterization of the soil moisture profile at the beginning of storm and interstorm events is a critical factor in water balance models based on physics-based infiltration and exfiltration relations. This report contains the results of detailed analyses of soil moisture dynamics carried out by numerical integration of the governing equations of moisture flow. The simulations consist of forcing a one-dimensional soil column, bounded at its base by a fixed water table, with a stochastic event based model of precipitation and potential evaporation. The simulations are designed to illustrate the role of temporal variability of soil moisture in the dynamics of runoff production and evaporation.

The results and conclusions are presented in two seperate but related works. The first uses perturbation analysis of the governing equations and the above described numerical simulations to demonstrate that the equivalent steady moisture profile, i.e. the unique steady moisture profile which transmits the longterm mean flow, forms a sufficient and practical estimate of the pre-storm and pre-interstorm moisture profiles. The utility of the approximation is demonstrated through comparison of the mean of simulated fluxes (infiltration and evaporation) with the flux predicted by a flux capacity-time compression model using the equivalent steady intitial condition. The comparison is favorable under both deep and shallow water table conditions. The same analysis is carried out for the commonly used approximation that pre-event moisture profiles are approximately hydrostatic. This assumption is shown to severely underestimate the near surface soil moisture, resulting in diminished exfiltration capacities and exaggerated infiltration capacities.

In the second section, a simple approximate analytic expression is derived for the steady-state profile in soils with realistic power law unsaturated hydraulic properties. The solution applies both to situations of recharge and capillary rise, and also contains the hydrostatic condition as a special case. As suggested above, this profile can then be used to initialize flux capacities by setting the steady flow parameter equal to the mean recharge, providing a simple analytic coupling between the saturated and unsaturated zones in water balance modelling.

Acknowledgements

This work has been supported by the National Aeronautics and Space Administration subcontract NAS 5-31721 and grant NAGW 1696. We also thank Dr. Peter S. Eagleson for his contributions to this work.

EQUILIBRIUM WATER BALANCE: THE ROLE OF THE SOIL MOISTURE PROFILE AND THE TIME COMPRESSION APPROXIMATION IN WATER BALANCE MODELLING

Guido Daniel Salvucci
Dara Entekhabi

Ralph M. Parsons Laboratory
Massachusetts Institute of Technology, Cambridge, MA., 02139

Abstract

The definition of pre-event soil moisture profile and time compression analysis are critical components in recent generation water balance models that are based on realistic infiltration/exfiltration relations and include profile-redistribution of vadose zone moisture. In this paper, detailed analysis of these two fundamental components of water balance modelling are presented. Numerical integration of the governing equations for liquid moisture flow in the unsaturated zone are used in simulations designed to illustrate the role of temporal variability in the system. The simulations consist of forcing the surface of a one-dimensional soil column, bounded at its base by a fixed water table, with the output of a stochastic event-based model of precipitation and potential evaporation. The simulations are run until and beyond when an equilibrium condition is reached between the long term mean of surface and bottom fluxes. For situations with deep water table, two distinct zones develop: a near surface highly unsteady zone and a deeper quasi-steady zone. The equivalent steady moisture profile, i.e. the steady profile corresponding to the mean of the simulated column flow, is found to reasonably approximate the temporal mean, mean pre-storm, and mean post-storm moisture profiles, particularly in the deeper zone. In the upper zone, the equivalent steady profile forms a biased estimate of the temporal mean. The bias is shown, through perturbation analysis, to lead to overestimation of the wetness of the mean moisture profile. For shallow water tables, the distinction between the two zones collapses. In this case, both the equivalent steady profile and the mean profile are nearly hydrostatic. The simulations are also used to test the utility of the time compression approximation (TCA) in modelling surface fluxes under temporally variable

initial conditions. We demonstrate that the use of the mean pre- and post- storm event moisture profiles as initial conditions for the infiltration and exfiltration flux capacities does not produce major bias in TCA predicted surface fluxes. In a certain sense, the TCA behaves as a linear operator. Furthermore, we demonstrate that the estimation of these mean initial condition profiles by the equivalent steady state soil moisture profile is an adequate approximation for determining landsurface response to event-based atmospheric forcing.

Introduction

Equilibrium water balance describes models and calculations that result in the determination of the partitioning of atmospheric forcing at the land surface. Atmospheric forcing refers to precipitation intensity during storm events and atmospheric evaporative demand (potential, or energy limited evaporation) during interstorm periods. The landsurface partitions this atmospheric forcing into infiltration, surface runoff, bare soil evaporation, transpiration, groundwater runoff and changes in storage. This partitioning depends on the state of the landsurface and the sequence and characteristics of atmospheric forcing events.

Since the landsurface water and energy balances are coupled through the latent heat of vaporization and inertia terms, the water balance partitioning has a strong influence on the determination of seasonal land climatology. The heat and moisture balance at the surface in turn influences the climatology and general circulation of the overlying atmospheric fluid. Thus both hydrologists and climatologists have focused effort on improving water balance estimation at the landsurface.

Depending on their particular goals, hydrologists have studied moisture fluxes both on short time scales (as in event predictions of flooding) and also on longer time scales (particularly for water resources planning). Climatologists have traditionally been concerned only with long term means (and their trends). Recent use of numerical models to simulate climate, however, has focused their interest in hydrology on much smaller temporal scales (e.g. hours). Furthermore, hydrologists have begun to recognize that some important water resources problems, such as drought persistence, may best be understood in the framework of coupled hydrology-climate models (Entekhabi et al., 1993).

In this work, we will address the climate water balance from a hydrologist point of view: i.e., a long term average of event time-scale additions to and subtractions from the moisture stored in the land surface. Because these exchanges depend both on the atmospheric forcing of the landsurface boundary and on the moisture stored in the unsaturated zone of the land surface, and because wetter moisture states cause the soil to evaporate and drain more readily, while drier states cause the opposite, the system is driven to a long term intermediate equilibrium state. The fluxes associated with this equilibrium moisture state form the climate water balance (Eagleson, 1978a). Note that this state dependence of the landsurface's response to atmospheric forcing introduces memory and nonlinearity into the system, making solution of the mean water balance non-trivial.

The main purpose of this paper is to develop insight into the relation of: 1) soil moisture profile dynamics, 2) the position of the water table, 3) the flux partitioning at the landsurface, and 4) the time compression approximation, which allows analytic solution under complex boundary conditions. The simulation experiments and the analyses are meant to serve as illustrative examples of physical processes.

Definition of hydrologic processes and their atmospheric forcing

In the following analysis, the hydrologic system and atmospheric forcing are represented as in Eagleson (1978a,b), except that vegetation is not considered in the analysis. This simplification is made in order to focus the current investigation, not to diminish its importance in water balance determination. In subsequent studies where we assemble an equilibrium water balance model, vegetation is included. We focus on a single, representative one-dimensional soil

moisture profile, instead of analyzing a full multidimensional and spatially inhomogeneous domain. Because the unsaturated zone dynamics are dominated by gravity and by moisture gradients whose steepest changes occur in the vertical (i.e. between the surface and the water table), we believe that this one-dimensional representation adequately captures the critical processes responsible for the system's response to the atmospheric forcing. This approximation has been partly supported by the work of Protopapas and Bras (1991), in which unsaturated flow solutions in a one dimensional domain were compared with solutions in a multidimensional domain of spatially non-uniform soil properties. In order to keep the focus of this analysis on the role of temporal variability, we take the soil properties to be homogeneous throughout the column. We do not expect that our results are particularly sensitive to this assumption because the spatial scale of variations in saturation (e.g. moisture fronts) are on the order of ten centimeters or less. The heterogeneity correlation scale is generally at this scale or larger and over this length scale the soils are relatively homogeneous.

Scaling the results from a one dimensional analysis to laterally-hydrologically connected and spatially inhomogeneous areas in order to yield information on the dynamics of area-averaged fluxes is a nontrivial task. A variety of approaches exist in the literature (c.f. Milly, 1988), their applicability depending mostly on the size of the area in question (e.g. Dagan and Bresler, 1983; Milly and Eagleson, 1987; Entekhabi and Eagleson, 1989 , Famiglietti and Wood., 1991a). A method appropriate to the hillslope scale, which incorporates the lateral redistribution of fluxes from the unsaturated zone by the saturated zone, is presented by Salvucci and Entekhabi (1993). Essentially, the method allows only lateral flows in the saturated zone and only vertical flows in the unsaturated zone, similar to the approach of available models (e.g. Abbot et al., 1986).

With these assumptions, we represent the land surface at a point by a one dimensional soil column bounded by a fixed water table at some depth ($-Z_w$). In the case studies presented here and in Salvucci and Entekhabi (1993), this depth is fixed at different values so that the effect of the presence of a shallow water table on the surface partitioning and profile dynamics can be studied.

Flow through this characteristic soil column is modelled with Darcy's law:

$$q = -K(\Psi)\frac{d\Phi}{dz} \qquad (1)$$

where

z = vertical Cartesian coordinate (cm), positive upward

q = flow rate (cm/sec) (positive for q in direction of z, i.e. evaporation)

$K(\Psi)$ = unsaturated hydraulic conductivity (cm/sec)

$\Psi(s)$ = capillary tension head (negative), (cm)

s = relative soil saturation (dimensionless) equal to the volume of water divided by the pore volume available to moisture flow.

Φ = total energy head

The total energy head (Φ) in the unsaturated zone is taken as the sum of the capillary pressure head (Ψ) and the gravitational head. Equation (1) then yields:

$$q = -K(\Psi)\cdot\left(\frac{d\Psi(s)}{dz} + 1\right) \qquad (2)$$

Applying continuity for a soil of effective porosity n, we find:

$$n \cdot \frac{ds(\Psi)}{dt} = -\frac{d}{dz}\left(-K(\Psi)\cdot\left(\frac{d\Psi(s)}{dz}+1\right)\right) \qquad (3)$$

which we take as the governing equation describing moisture flow.

There are a multitude of models for relating capillary tension, unsaturated conductivity, and soil saturation. In this analysis we incorporate the Brooks-Corey (1966) model, which is simple in form and represents the behavior well over a large range of soil textures. The model equations are given in the Appendix. Note that, as pointed out by Philip (1969), the governing equation should be left in this "Ψ" based form if the soils being modelled have tension-saturated zones, as in the Brooks-Corey model.

Equation (3) is solved using the numerical finite element program developed by Milly (1982), subject to stationary event-based atmospheric forcing. This forcing ($q_o(t)$) acts in conjunction with tension state at the soil surface to yield the following (state dependent) boundary conditions:

for $q_o(t)$ negative (rainfall):

$$-K(\Psi(s)|_{z=0})\cdot\left(\frac{d\Psi(s)}{dz}|_{z=0}+1\right) = q_o(t) \qquad \text{if } \Psi(s)|_{z=0} < 0 \qquad (4)$$

$$\Psi(s)|_{z=0} = 0 \qquad \text{if } -K(0)\cdot\left(\frac{d\Psi(s)}{dz}|_{z=0}+1\right) > q_o(t) \qquad (5)$$

for $q_o(t)$ positive (evaporation):

$$-K(\Psi(s)|_{z=0}) \cdot \left(\frac{d\Psi(s)}{dz}|_{z=0} + 1 \right) = q_0(t) \quad \text{if} \quad \Psi(s)|_{z=0} > \Psi_{min} \quad (6)$$

$$\Psi(s)|_{z=0} = \Psi_{min} \quad \text{if} \quad -K(\Psi_{min}) \cdot \left(\frac{d\Psi(s)}{dz}|_{z=0} + 1 \right) < q_0(t) \quad (7)$$

Summarizing Equations (4) and (5), the switching of the boundary condition from a flux condition to a Ψ condition occurs whenever Ψ at the soil surface reaches zero, at which time the water is assumed free to "run off" (i.e. surface retention is neglected). Likewise in Equations (6) and (7), the switching occurs whenever Ψ at the surface reaches the (large) negative value (Ψ_{min}) at which it is in thermodynamic equilibrium with the near surface atmospheric moisture (Gardner, 1959).

When the soil can absorb (or yield) moisture at the rate which the overlying atmosphere provides (or demands), as in Equation (4) and (6), the system is said to be "climate" controlled. This condition occurs at the onset of a rainfall or evaporation period, and applies until the surface either dries to Ψ_{min}, or wets to $\Psi = 0$. This switching may or may not ever occur, depending on the sequence and nature of the forcing, the antecedent moisture state, and the soil characteristics. If and when it does occur, Equations (5) and (7) govern at the boundary and the system is referred to as "soil" controlled or "profile" controlled. The soil controlled periods are responsible for infiltration-excess Hortonian surface runoff production and for actual less than potential evaporation.

Note that if the boundary conditions were not state dependent, the solution of the long term mean water balance would be trivial, i.e. the mean annual yield would simply equal the mean annual precipitation minus the mean annual potential evaporation. Absent the effects of vegetation and snow, this nonlinear interaction of the forcing and the surface moisture state to form the soil-atmosphere boundary condition is the key to the partitioning of the climatic forcing of precipitation and evaporative demand into infiltration, runoff, recharge and evaporation.

The climate forcing, $q_o(t)$, is modelled as a stochastic process consisting of the Poisson arrivals of storm pulses which last for an exponentially distributed duration (t_r). Over this duration, it rains at an intensity (i), also taken as an exponentially distributed random variable. The Poisson storm arrivals imply an exponential distribution of the time between storms (t_b), during which the potential evaporation (e_p) defines the atmospheric forcing at the landsurface. We will refer to these storm pulses and interstorm evaporation periods as "events".

This is essentially the "event based" stochastic forcing used in Eagleson's (1978c) equilibrium water balance model. While clearly an approximation, this forcing process retains those variables which are important to the dynamics of runoff production and interstorm exfiltration. Most importantly, it realistically models event variability and extremes which often place the system under "soil" control.

In what follows, we present some observations of different properties of the moisture profile, flux rates and water balance dynamics which we derived from "monte-carlo" solutions of the above described unsaturated flow system. These observations lead us to a set of conclusions regarding the utility and accuracy of various approximations commonly used in water balance modelling.

Case studies for moisture profile analysis

Two case studies are presented, one with a deep and one with a shallow water table. For both cases, the climate is characteristically semi-humid. The storm structure parameters (Table I) were estimated based on Hawk's (1992) results for Savannah Georgia and the potential evaporation was estimated based on regional lake evaporation (Bras, 1990). The Brooks-Corey soil parameters (Table II) listed are typical of clay soils (Bras, 1990). We found this combination to yield enough "soil controlled" events to be illustrative of the interactive nature of the atmospheric forcing on the land surface. Salvucci and Entekhabi (1993) extend the analysis to other climates and soil textures.

For the two cases, Milly's (1982) unsaturated flow code was used to simulate twenty years of moisture profiles. Each twenty year simulation contained approximately 4,000 "events" (2,000 rainstorms and 2,000 "interstorms"). In these simulations, the moisture profile at the end of one event (e.g. a period of rain) is used as the initial condition for the next event (e.g. an interstorm period of evaporation).

The long term mean water balance for each case is presented in Table III. The mean annual surface fluxes (evaporation and infiltration) and bottom flux (recharge or capillary rise) were found by integrating the surface and bottom flux rates throughout the simulation.

For the deep water table case, which might represent a point in the watershed far from a channel, the actual evaporation is approximately eighty percent of the potential evaporation and about four percent of the precipitation became surface runoff. This is the result of the "soil controlled" periods in the simulation. For the shallow water table case the near surface moisture state is much wetter, yielding more surface runoff, and evaporation equal to the potential

TABLE I: CLIMATE PARAMETERS

representative climate	Savannah, Georgia
mean storm intensity (m_i)	5.07 (cm/day)
mean storm duration (m_{tr})	0.25 (days)
mean annual potential evaporation (e_p)	120.45 (cm)
mean interstorm duration (m_{tb})	3.44 (days)
mean annual precipitation (mP_a)	125.4 (cm)

TABLE II: SOIL PARAMETERS

representative soil	Clay
saturated hydraulic conductivity (K_S)	2.94 (cm/day)
bubbling tension head (Ψ_S)	-90 (cm)
porosity (n)	0.45
pore size distribution parameter (m)	0.44

TABLE III: SIMULATED MEAN ANNUAL WATER BALANCE

(all values in centimeters)

	CASE I	CASE II
water table depth (Z_w)	750	150
precipitation (mP_a)	124.65	124.65
evaporation (mE_a)	88.29	112.36
surface runoff (mR_{sa})	4.73	23.99
exchange with saturated zone (mR_{ga})	31.84	-12.02

evaporation. In this shallow water table case, which might be representative of a near-channel point in a watershed, the mean bottom flux is extracting moisture from the saturated zone. In a watershed or along a hillslope this could correspond to a region of groundwater discharge, in which case the saturated zone's losses would be replenished by recharging areas (e.g. the "far-channel", deep water table point in case I).

Moisture profiles under deep water table conditions

In Figure 1, five important characteristics of the simulated moisture profile are plotted: 1.) the temporal mean profile (solid line); 2.) the mean of all the profiles at the beginning of each storm event (dashed line); 3.) the mean of all the profiles at the end of each storm event (beginning of interstorm event; dotted line); 4.) the hydrostatic profile (dot-dashed line; i.e. the steady, zero flow profile); and 5.) the "equivalent steady state" profile (long dashed line; i.e. the steady state profile that would exist if the boundary condition at the surface were held constant at the mean recharge rate, e.g. 31.8 cm/yr, Table III). The significance of the mean pre-storm and mean post-storm profiles is that they represent the mean initial condition for storm rainfall and interstorm evaporation events. As one would expect, the mean profile after rainstorms is wetter than the profile that serves as the initial condition for the storm event. The difference is contained in the top fifty centimeters that is affected by the infiltration front. Note that the temporal mean profile is approximately equal to the mean pre-storm (post-evaporation) profile, indicating that during evaporation the soil profile "redistributes" its previous wave of infiltrated moisture rapidly. Most importantly note that the equivalent steady profile forms a good estimate of the other profiles, particularly in the deeper soil. This is due, in part, to the damping

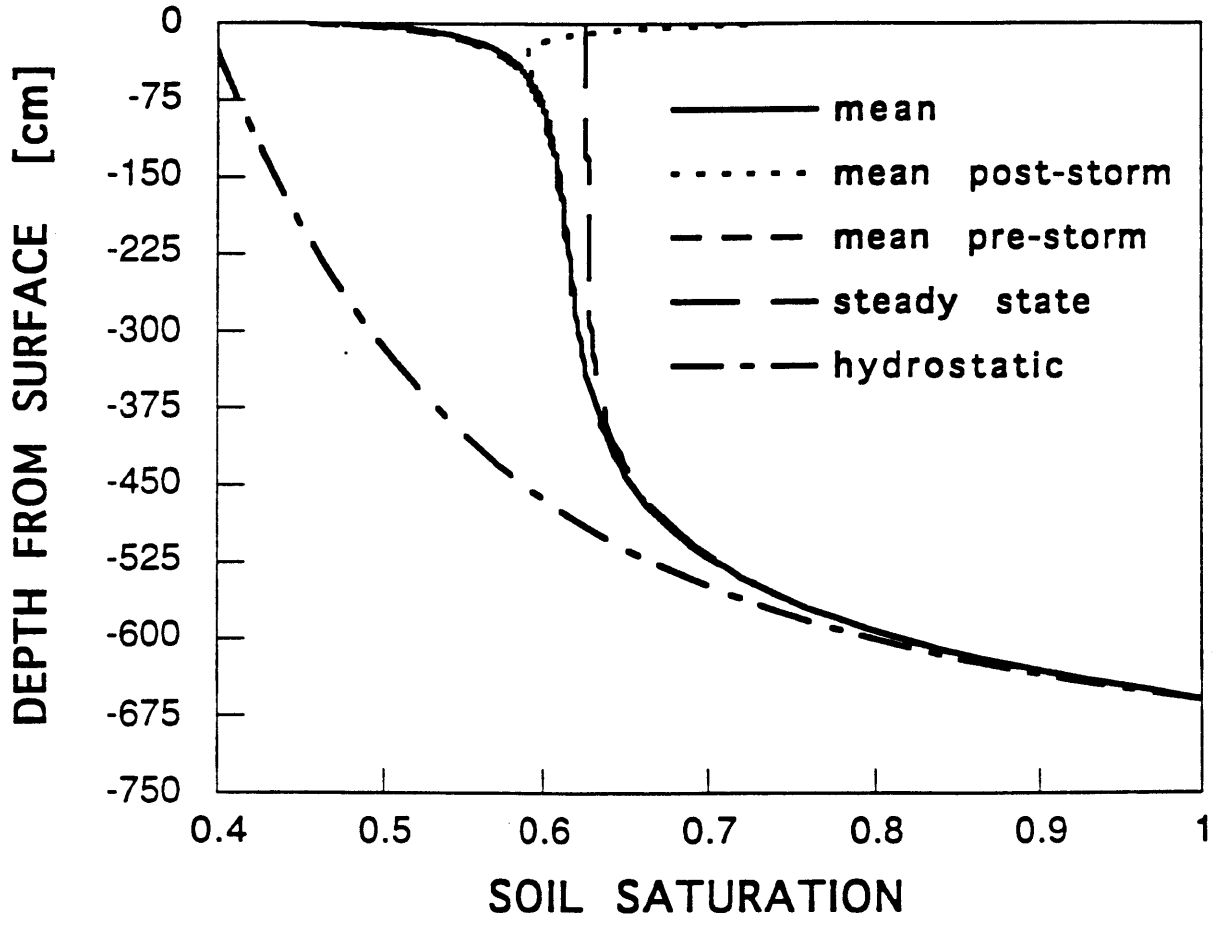

Fig. 1. Characteristic moisture profiles: Deep water table case

out of surface forcing induced perturbations with depth. For the linearized diffusion equation, this damping can be shown, by harmonic analysis, to be exponential with depth with the e-folding rate dependent on the frequency of changes in the boundary condition (cf. Carslaw and Jaeger, 1989, p. 389). In general, lower frequency fluctuations penetrate deeper. We would thus expect that seasonal changes, had we modelled them in our forcing, would penetrate deeper, causing more deviation between the equivalent steady and mean profiles. The hydrostatic profile will be discussed in the final section of this paper.

To illustrate the relation between the equivalent steady profile and the temporal mean profile, consider the case of "exponential" soils (see Appendix). For this representation of soil properties the darcy flux equation is linear (the diffussivity is constant and the gravity term depends on s linearly) :

$$q = -\frac{K_S}{\alpha}\left(\frac{ds}{dz}\right) - K_S \cdot s \qquad (8)$$

If we now express the soil moisture and flux rate as a temporal mean (<( )>) plus a perturbation (( )'), we can write (8) as:

$$\langle q \rangle + q' = -\frac{K_S}{\alpha}\left(\frac{d\langle s \rangle}{dz} + \frac{ds'}{dz}\right) - K_S \cdot (\langle s \rangle + s') \qquad (9)$$

Because of the linearity of (8), taking the mean of Equation (9) yields no covariance terms, i.e. the mean equation is simply:

$$\langle q \rangle = -\frac{K_S}{\alpha}\left(\frac{d\langle s \rangle}{dz}\right) - K_S \cdot \langle s \rangle \qquad (10)$$

For the linear case then, the mean moisture profile will be identical to the steady state solution for the mean flow through the column.

For the Brooks-Corey soil model, the darcy flux is nonlinear:

$$q = \frac{K_S \cdot \Psi_S}{m} s^{(c+1)/2}\left(\frac{ds}{dz}\right) - K_S \cdot s^c \qquad (11)$$

Again we express the soil moisture and flux as a temporal mean plus a perturbation, expand the nonlinear terms around <s> and average the resulting equation. The mean and perturbation equations now become coupled by covariance terms, similar to the classical "closure" problem in turbulence:

$$\begin{aligned}\langle q \rangle = {} & K_S \cdot \Psi_S \frac{c-3}{2} \langle s \rangle^{(c+1)/2}\left(\frac{d\langle s \rangle}{dz}\right) - K_S \cdot \langle s \rangle^c \\ & + \frac{1}{4} K_S \cdot \Psi_S (c+1)(c-3) \langle s \rangle^{(c-1)/2} \left\langle s' \cdot \frac{ds'}{dz} \right\rangle\end{aligned} \qquad (12)$$

Note that a perturbation increasing q (e.g. a strong evaporation event) dries the soil, making $s' < 0$, from the surface down, making $ds'/dz < 0$. A perturbation decreasing q (e.g. an infiltration event) wets the soil ($s'>0$) from the surface down ($ds'/dz > 0$). The covariance term in Equation (12) is thus positive and therefore the mean profile is always drier than the equivalent steady state profile. In Figure 1 the deviation between the mean and steady state profiles increases closer to the surface where the magnitudes of the q and s fluctuations and covariance are largest.

In summary, for a "linear" soil, the equivalent steady moisture profile is identical to the mean profile, while for a "nonlinear" soil, the equivalent steady

profile forms a "zeroth" order (i.e. disregarding the covariance term) estimate of the mean.

The damping of fluctuations by the diffusive process can be seen in the temporal variance of the flux around the mean state at various depths. In Figure 2, for a range of depths, the cumulative variance of q is shown for perturbations with period two hours to approximately one year. The asymptotic values of these cumulative power spectrum curves are the total variance of the flow for various depths. The asymptotic values indicate rapid total variance reduction with depth. For example, flow at the 72 cm. depth shows two orders of magnitude less variance than at the surface. More importantly, note that the near surface variability is mostly contained in the high-frequency event scale range, while the flow variability in the deeper soil comes from low-pass filtered fluctuations. At the event scale, for example, the variability is reduced by two orders of magnitude over only 31 centimeters, less than half the distance required for the total variance. For the purpose of event time scale modelling, we may then assume that the moisture state and moisture flow below the near surface is in a quasi-steady state.

This structure of moisture and flux profile variability suggests that the column can be broken up conceptually, and for modelling purposes (e.g. Eagleson, 1978c), into two characteristic zones: a highly unsteady near surface zone and a deeper quasi steady zone. In the lower zone the equivalent steady state profile is an adequate estimate of the actual profile at any time. In the upper zone it gives a zeroth order estimate of the temporal mean, mean pre-storm, or mean post-storm profile. If we measure the value of this estimate in terms of its bias and variance, then the "equivalent steady profile" estimate is seen to improve with depth on both accounts.

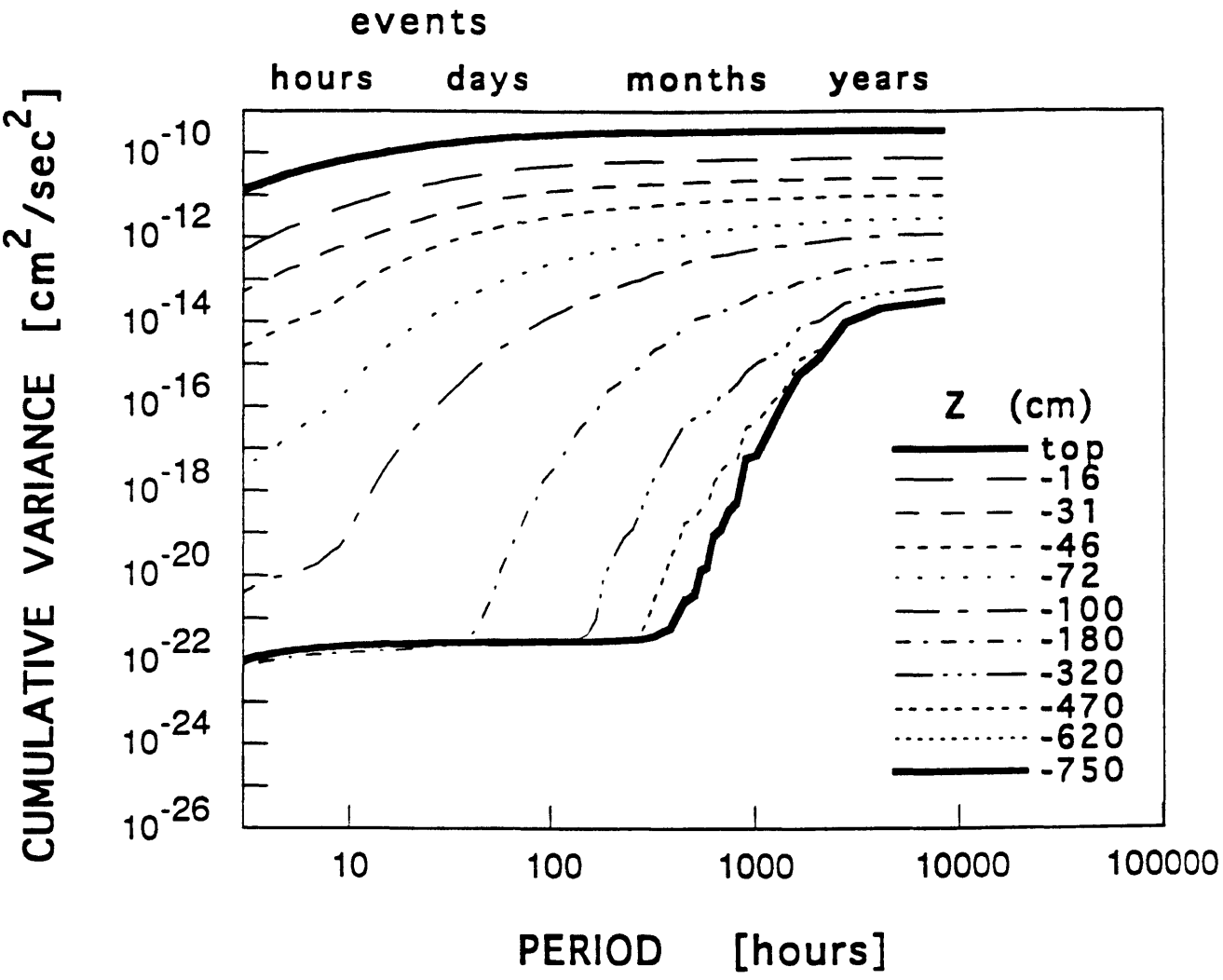

Fig. 2. Cumulative power spectra of flow variability at various depths: Deep water table case

Moisture profiles under shallow water table conditions

For a soil column bounded by a shallow water table, the moisture profiles display some different properties. Note in Figure 3 that the equivalent steady profile (dashed line) is a much better estimate of the temporal mean profile (solid line) than in the deep water table case, and that beyond the tension saturated zone the mean, steady state, and pre-storm moisture profiles are approximately linear. This is because near the water table, where the soil is relatively wet and near saturation, the soil has high unsaturated conductivity relative to typical forcing rates (e.g. $e_p/K_S \sim 0.1$). Darcy's law (Eq. 2) then implies that only small deviations from a hydrostatic profile are necessary to balance typical perturbations in the atmospheric forcing. Thus for nearly saturated soils, in which the moisture content locally scales near linearly with Ψ, the moisture profile will increase linearly with z.

In summary, either the equivalent steady profile or the hydrostatic profile form an accurate estimate of the temporal mean and mean pre-storm profiles. The mean post-storm profile (dotted line, Fig. 3) deviates by a considerable amount, but since the soil is thoroughly moist in this shallow water table case, the interstorm evaporation will proceed at the potential rate, making specification of the pre-interstorm initial condition profile irrelevant.

Note that the profile in this shallow case can no longer be conceptually divided into a highly unsteady zone and quasi-steady zone. This is also evident in the cumulative power spectra (Fig. 4). For this case, there is less reduction in total variance with depth and more importantly, the reduction is not dependent on frequency. For example the zero depth and bottom depth curves run roughly parallel over most frequencies, indicating that they are picking up variance from the same frequency perturbations. The importance of these differences will be

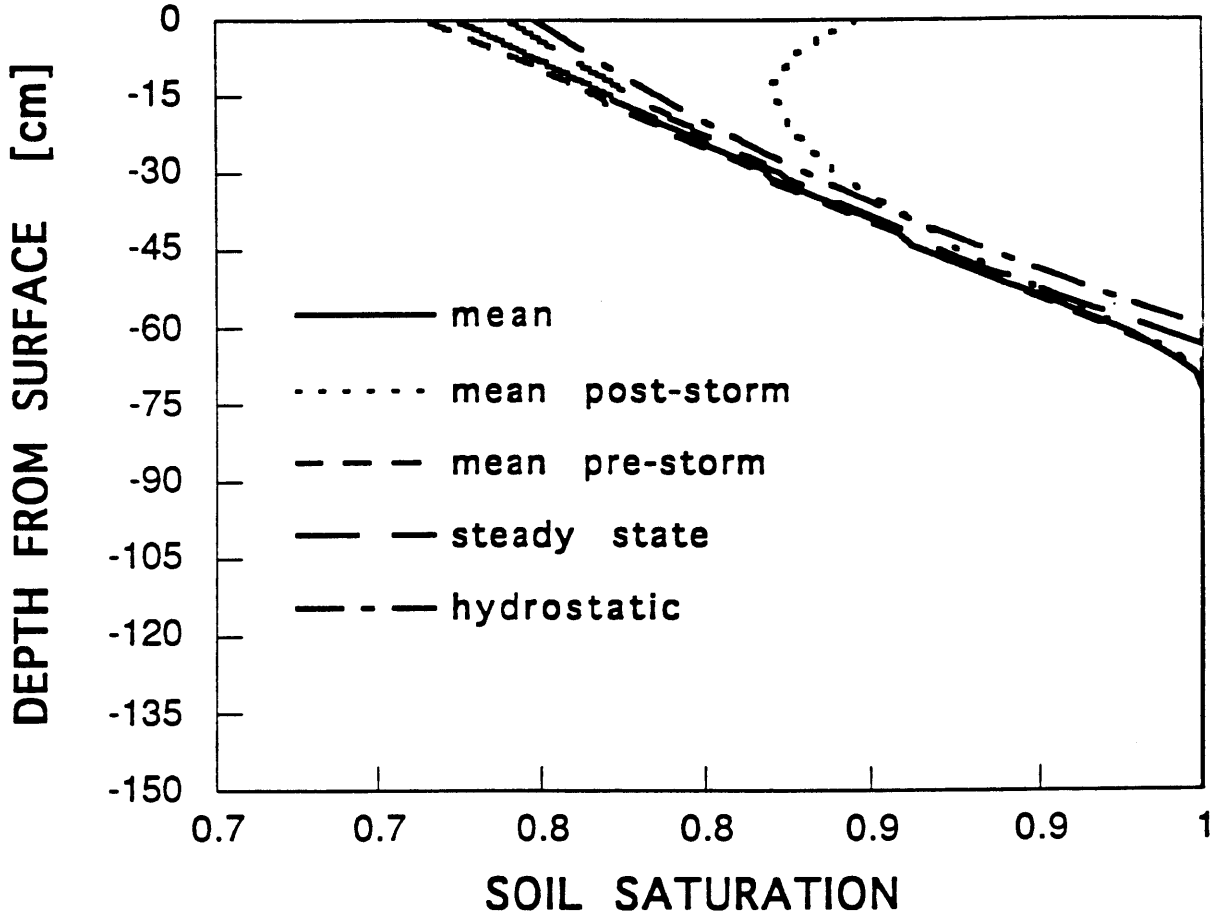

Fig. 3. Characteristic moisture profiles: Shallow water table case

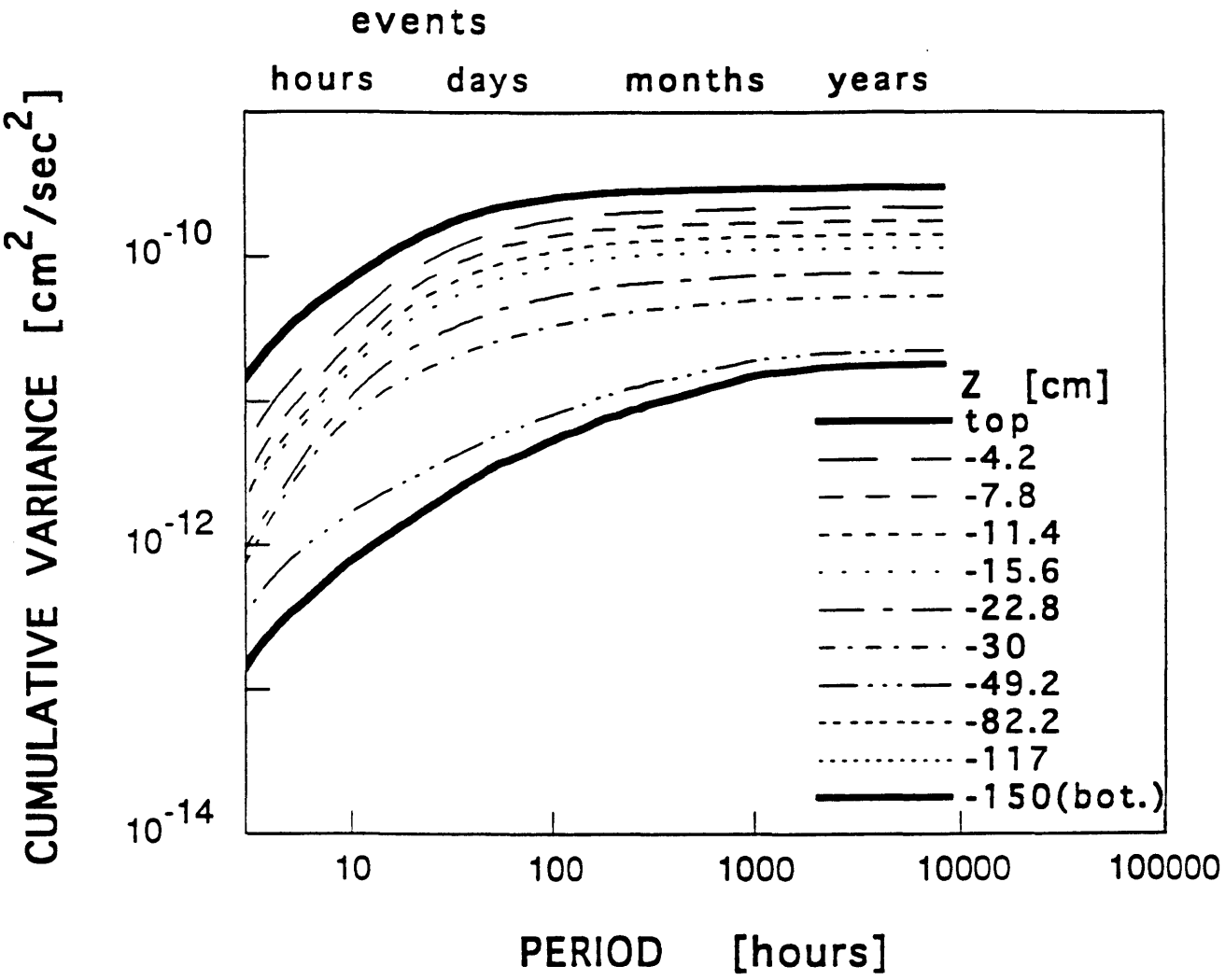

Fig. 4. Cumulative power spectra of flow variability at various depths: Shallow water table case

discussed in the final section of this paper and in the Salvucci and Entekhabi (1993).

One of our central conclusions is that even for soils with nonlinear diffusivity, the equivalent steady flow moisture profile is a sufficient estimate of the mean initial condition profile for both infiltration events (e.g. as represented by the mean before storm profile) and exfiltration events (as represented by the mean after storm profile). Part of the reason for this is that the soil controlled periods of infiltration and exfiltration events are more dependent on the moisture state of the deeper soil, where the equivalent steady profile estimates the pre-event profiles with the least bias and variance. This is an important proposition and we will demonstrate it with the use of time compression analysis.

Time compression analysis

Time compression analysis (TCA) is a commonly used approximation in water balance modelling (e.g. Reeves and Miller, 1975; Eagleson, 1978; Milly, 1986; Smith and Hebert, 1983; and Smith et al., 1993). It is derived from an assumption that the maximum rate at which a soil column can infiltrate or exfiltrate water (the infiltration/exfiltration "capacity") at any given time during an event depends only on the initial moisture state of the column and the cumulative moisture exchange up to that time. The concept was first used in the context of infiltration by Sherman (1943; referenced in Sivapalan and Milly, 1989) and in the context of exfiltration by Philip (1957b). The utility of the approximation is that, for a given initial moisture state, one can use a single characteristic capacity curve, derived as the solution to the infiltration (or exfiltration) rate under "flooded" (or extremely dry) surface concentration boundary conditions, to model the surface flux rate, even if the boundary is

actually governed by a combination of flux (i.e. rainfall intensity, before ponding) and head (i.e. $\Psi = 0$, after ponding) conditions. Sivapalan and Milly (1989) discuss the relation of this approximation to the more rigorously defined "flux concentration relation" and use the latter to demonstrate the errors associated with the TCA. In general, they found that the validity of the approximation increases for soils whose diffussivities are highly nonlinearly dependent on soil moisture, becoming exact for Green-Ampt (delta function diffussivity) soils.

The following review applies to both infiltration (subscripted "i") and exfiltration (subscripted "e") but will be illustrated for infiltration only. First define the potential infiltration capacity as the maximum rate of infiltration into a given soil with some initial moisture profile $s_o(z)$, i.e. it is the rate of infiltration resulting from a continuously ponded surface. We denote this potential capacity by $f_i^*(t;s_o(z))$, and its time integral, the potential cumulative infiltration, by $F_i^*(t;so(z))$. The infiltration capacity during an event which has not had a continuously ponded surface will be denoted the event infiltration capacity, $f_{i,event}^*(t;s_o(z))$. This is the rate at which infiltration would occur if, at some time during an event under flux boundary conditions, the surface were ponded.

The time compression approximation states that the relation defined by mapping the potential infiltration capacity, $f_i^*(t;s_o(z))$ to the potential cumulative infiltration $F_i^*(t;s_o(z))$, will be approximately the same as the relation between the event infiltration capacity $f_{i,event}^*(t;s_o(z))$ and the cumulative event infiltration ($F_{i,event}(t;s_o(z))$). If we express this mapping as some function G^{tca}, defined by:

$$f_i^*(t;s_o(z)) \equiv G^{tca}\left(F_i^*(t;s_o(z))\right) \qquad (13)$$

then, by the time compression approximation, we may write:

$$f^{*}_{i,event}(t;s_o(z)) = G^{tca}\left(F_{i,event}(t;s_o(z))\right) \qquad (14)$$

Because the surface flux rate that will occur at the moment of ponding will be equal to the event infiltration capacity, the surface boundary conditions given by Equations (4) and (5) are equivalent to stating that the actual surface flux during an event, $f_{i,event}(t;s_o(z))$, will be the lesser of the event infiltration capacity ($f_{i,event}^{*}(t;s_o(z))$) and the event rainstorm intensity (i), i.e.:

$$f_{i,event}(t;s_o(z)) = MIN\left(f^{*}_{i,event}(t;s_o(z)),i\right) \qquad (15)$$

With (15), we may now find the cumulative event infiltration as:

$$F_{i,event}(t;s_o(z)) = \int_0^t f_{i,event}(\tau;s_o(z))\,d\tau \qquad (16)$$

For a given intial condition ($s_o(z)$), equations (13) through (16) implicitly relate the actual infiltration rate under any rainstorm intensity (i) to the single characteristic potential infiltration capacity curve found under continuously ponded conditions.

All that remains is to determine the relation $f_i^{*}(t;s_o(z))=G^{tca}.(F_i^{*}(t;s_o(z))$. This can be found either by field experiment, by numerical simulation, or analytically, if one has an exact or approximate infiltration equation for the

continuously flooded boundary condition. For the initial condition $s_o(z)$ constant with depth, many such expressions exist (e.g. for infiltration: Philip, 1957a; Green and Ampt, 1911, referenced in Hillel, 1980; and Haverkamp et al., 1990; and for exfiltration: Eagleson, 1978c).

With one of the above numerical, experimental, or analytic solutions, the time compression approximation may be simplified into either a time based equation, by eliminating the dependence on cumulative infiltration, or as a cumulative infiltration based equation, by solving out time (e.g. Milly, 1986). We will follow the time based method.

First note that the event infiltration capacity is, by definition, equal to the forcing (i) at the time of ponding (t_p):

$$f^*_{i,event}\left(t_p ; s_o(z)\right) = i \tag{17}$$

Now define a compression time, t_c, as the time when the potential infiltration capacity is also equal to the forcing, i.e:

$$f^*_i\left(t_c ; s_o(z)\right) = i \tag{18}$$

By the TCA postulate (Eq. 13 and 14), these two capacities are only dependent on the cumulative infiltration and the initial condition, thus:

$$F_{i,event}\left(t_p ; s_o(z)\right) = F^*_i\left(t_c ; s_o(z)\right) \tag{19}$$

Because the two capacities only depend on the cumulative infiltration, and because their cumulative infiltrations are identical at time t_p and t_c, the flux capacity at equal increments after these times will also be identical, i.e.:

$$f^*_{i,event}\left(t_p + \tau; s_o(z)\right) = f^*_i\left(t_c + \tau; s_o(z)\right) \qquad (20)$$

Defining the time (t) to start at the beginning of an event, (20) and (15) yield our final expression for the time compression approximation of the event flux :

$$f_{i,event}(t; s_o(z)) \cong f^{tca}_i(t; s_o(z)) = \begin{cases} i & t<t_p \\ f^*_i\left((t-(t_p-t_c)); s_o(z)\right) & t\geq t_p \end{cases} \qquad (21)$$

In the above, t_c may be found from (18) and t_p may be found from (19) by noting that for $t < t_p$, $F_{i,event}$ is simply equal to the product of i and t_p and thus:

$$t_p \approx \left(\frac{1}{i}\right) \cdot \int_0^{t_c} f^*_i(\tau; s_o(z))\, d\tau \qquad (22)$$

Equations (18), (21) and (22) form the TCA approximation to the actual surface flux for any flux boundary condition i (or e_p), in terms of a single solution for the flooded (or extremely dry) concentration boundary condition.

Note that this set of equations (18, 21 and 22) retains the dependence of the surface flux on the initial condition moisture profile $s_o(z)$. The role of the initial condition in governing the potential for runoff and evaporation is, therefore, incorporated. For example, under conditions of wet initial moisture profile: 1.) the potential infiltration capacity ($f_i^*(t;s_o(z))$ is lower and the ponding time is shortened, thus enhancing (Hortonian) runoff production; and 2.) the potential exfiltration capacity is larger and the drying time (t_d) is lengthened, thereby

increasing the "climate" controlled fraction of the interstorm and increasing evaporation. Through this dependence two important factors in determining water balance are preserved, that of memory and that of state dependent, threshold switching of surface flux control from "climate" to "soil".

Test of the TCA approximation under uniform initial conditions

The accuracy of the time compression approximation for conditions of uniform initial moisture content is illustrated for both infiltration and exfiltration in Figures (5) and (6). The infiltration example was found using the clay soil of Table I and a (constant) intensity rainfall of five times the saturated conductivity, or approximately 0.6 cm hr^{-1}. The evaporation example uses the same soil and the potential evaporation from the case studies (Table I). The results show how well the TCA flux rates approximate the actual (mixed boundary condition) flux rate for the given atmospheric forcing. In each case the actual surface flux rate (solid line, found by numerical simulation) is shown with a time origin of zero, while the capacity (also found by numerical simulation) is shown both with a time origin of zero (triangles) and with its origin shifted by t_p-t_c (circles) (as determined by Equations (18) and (22)). The TCA flux rate solution would then be the rainfall intensity for $t < t_p$, and the shifted capacity curve (circles) for $t > t_p$, while for exfiltration it would be the potential evaporation (e_p) for $t < t_d$, and the shifted capacity curve for $t > t_d$. The approximation is remarkably accurate for infiltration.

Recently Poulovassilis et al (1991) suggested that the approximation is exact for conditions of infiltration into a soil of uniform initial soil moisture. This is inconsistent with the findings of Sivapalan and Milly (1989). In addition, Dooge and Wang (1993) have analytically demonstrated that the TCA cannot be

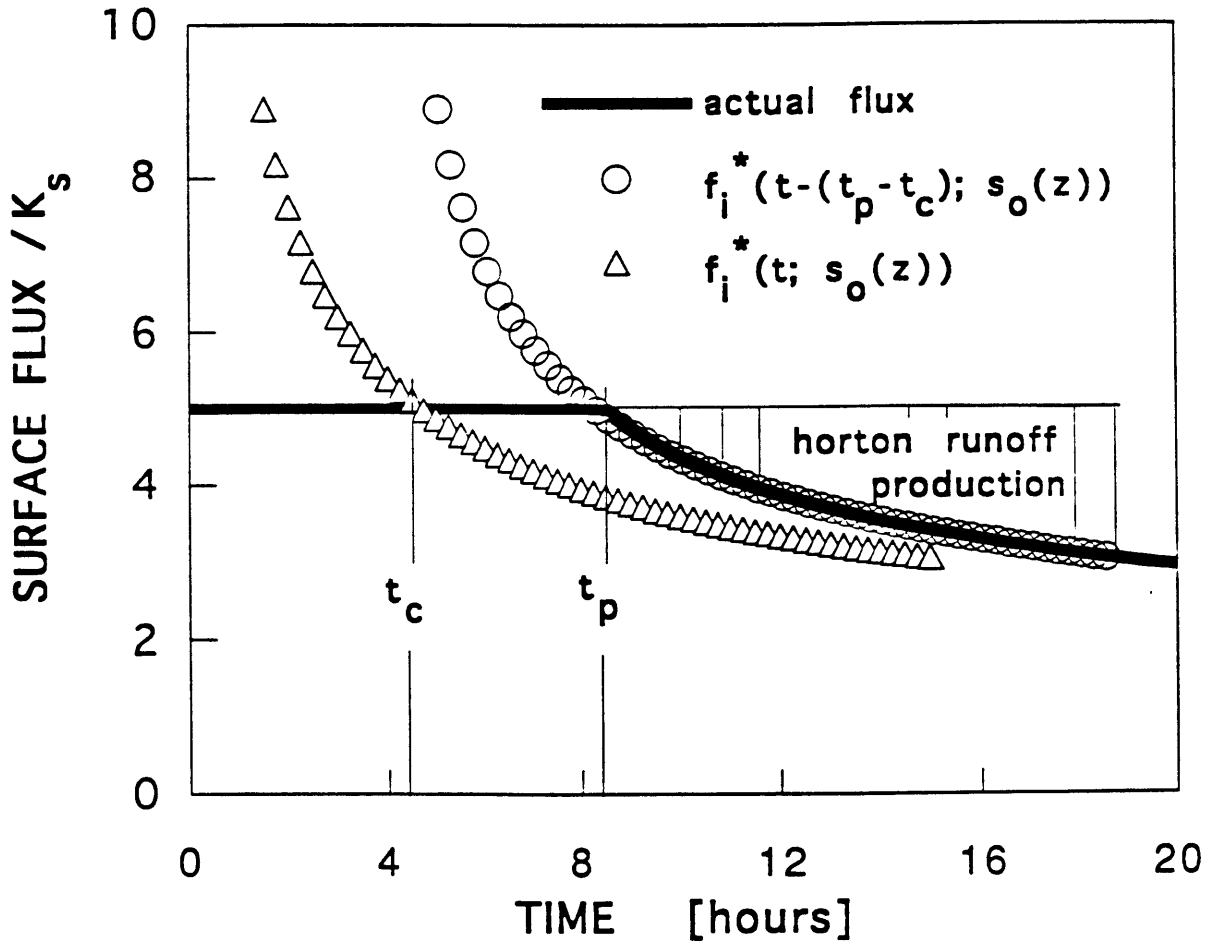

Fig. 5. Illustration of time compression approximation (TCA) for infiltration

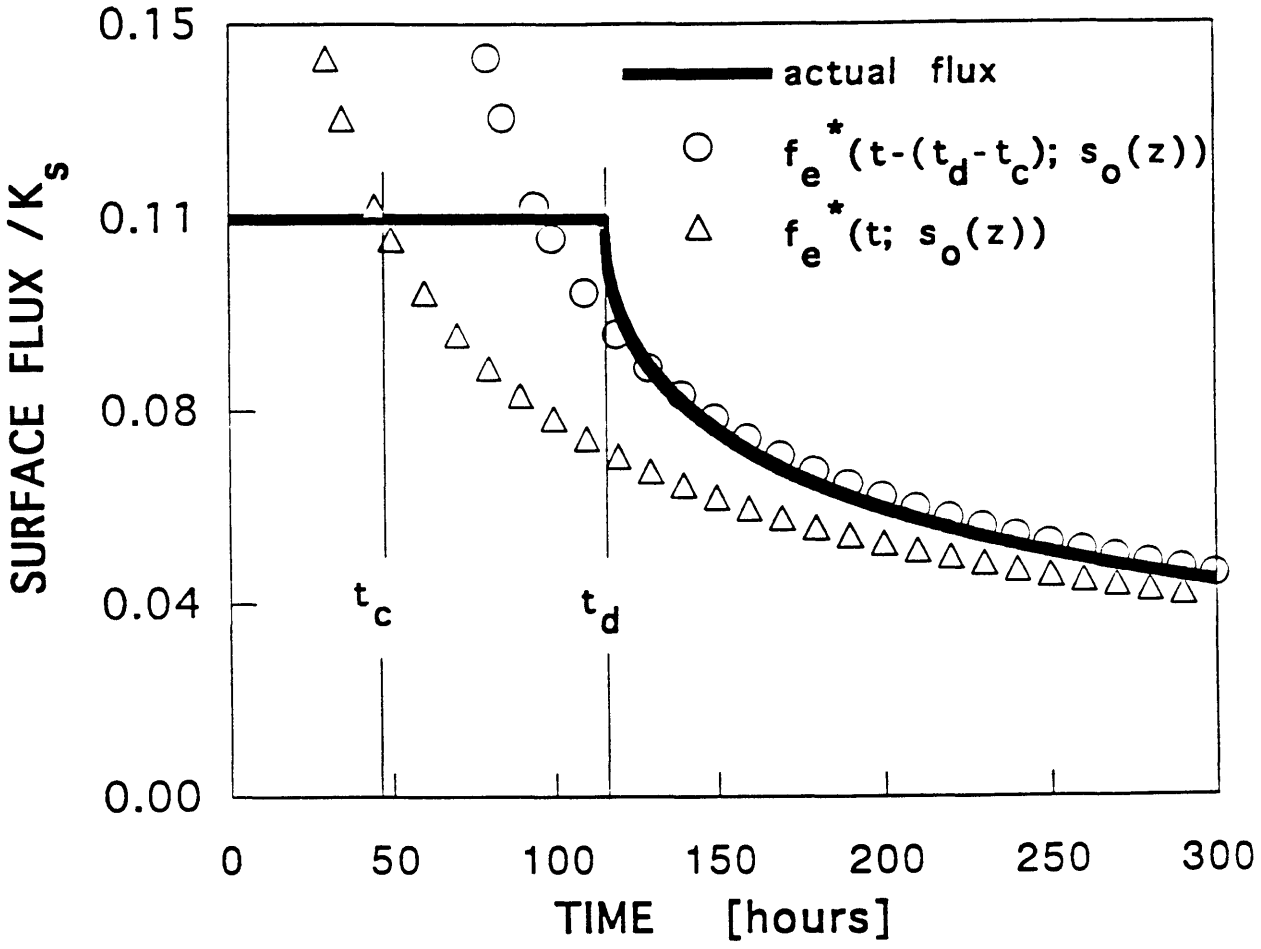

Fig. 6. Illustration of time compression approximation (TCA) for exfiltration

exact, but it is an excellent approximation for a large class of soil hydraulic property models.

Regardless of whether the TCA, under these conditions, is exact or just a very good approximation, the existence of a uniform moisture content at the beginning of a storm or interstorm is improbable and unrealistic. An important question then is: how well does the TCA holds up under various estimates of pre-event initial conditions? In the following Section, we use the results of the two case studies to address this issue.

Test of the TCA under mean initial conditions

For testing the applicability of the TCA to equilibrium water balance modelling and for determining its sensitivity to the initial condition moisture profile, we use the simulated moisture profiles from the previous two case studies as initial conditions. Because the stochastic atmospheric forcing used reasonably captures the important dynamics of real atmospheric forcing (Eagleson, 1978c), we expect that the variability of the simulated moisture profiles from one event to the next will be representative of the scale of (temporal) variability in the field.

For modelling the equilibrium water balance, an important test is to determine whether or not the infiltration or exfiltration capacity curves can be based on the mean initial condition of all events, and then used in a TCA analysis to reproduce the mean of the soil controlled surface fluxes. In essence, if the TCA behaves as a linear operator, one would expect this approximation to be adequate.

To test this for infiltration, we take pre-storm moisture profiles from the simulation results, and use each of them as the initial condition for simulating a

characteristic infiltration-excess runoff producing event. We then take the average of the one hundred profiles, and use this average ($<s_o(z)>$) as the initial condition to numerically simulate the capacity curve, f_i^* ($t; <s_o(z)>$). The average of all the simulated flux rate histories are then compared with the TCA approximated solution, using this "mean initial condition" capacity curve in (18), (21) and (22).

Figures 7 and 8 illustrate the results for the infiltration case under deep and shallow water table conditions. The applied flux rate for these examples is the same as that used in the uniform initial moisture profile test (i.e. 0.61 cm/hr). This rainfall intensity is chosen to illustrate the important concepts during transitions from climate-controlled to soil controlled conditions and not because it is typical. It is in fact relatively high in comparison with the mean intensity used in the case study (0.21 cm/hr, Table I), and would thus, on the basis of the assumed exponential distribution, occur for only about 6 percent of the storms. It is these "extremes" (i.e. $i>>K_s$), however, which produce Hortonian infiltration-excess runoff, and thus determine the departure of infiltration from mean precipitation.

The circles in the figures represent the TCA solution formed using the mean initial condition profile in the determination of the capacity curve. The solid lines represent the ensemble average of the (numerically simulated) flux histories, and the dashed lines show plus and minus one standard deviation of the flux rate around this mean. Note that the variation around the mean is least at early and late times. This is to be expected because: 1.) few post-evaporation moisture profiles (i.e. the infiltration initial conditions) are so wet as to cause very early ponding, and thus the early time solutions are soil independent ("climate controlled"); and 2.) at very late times, the near surface initial condition has been passed over by the infiltration front, leaving the flow

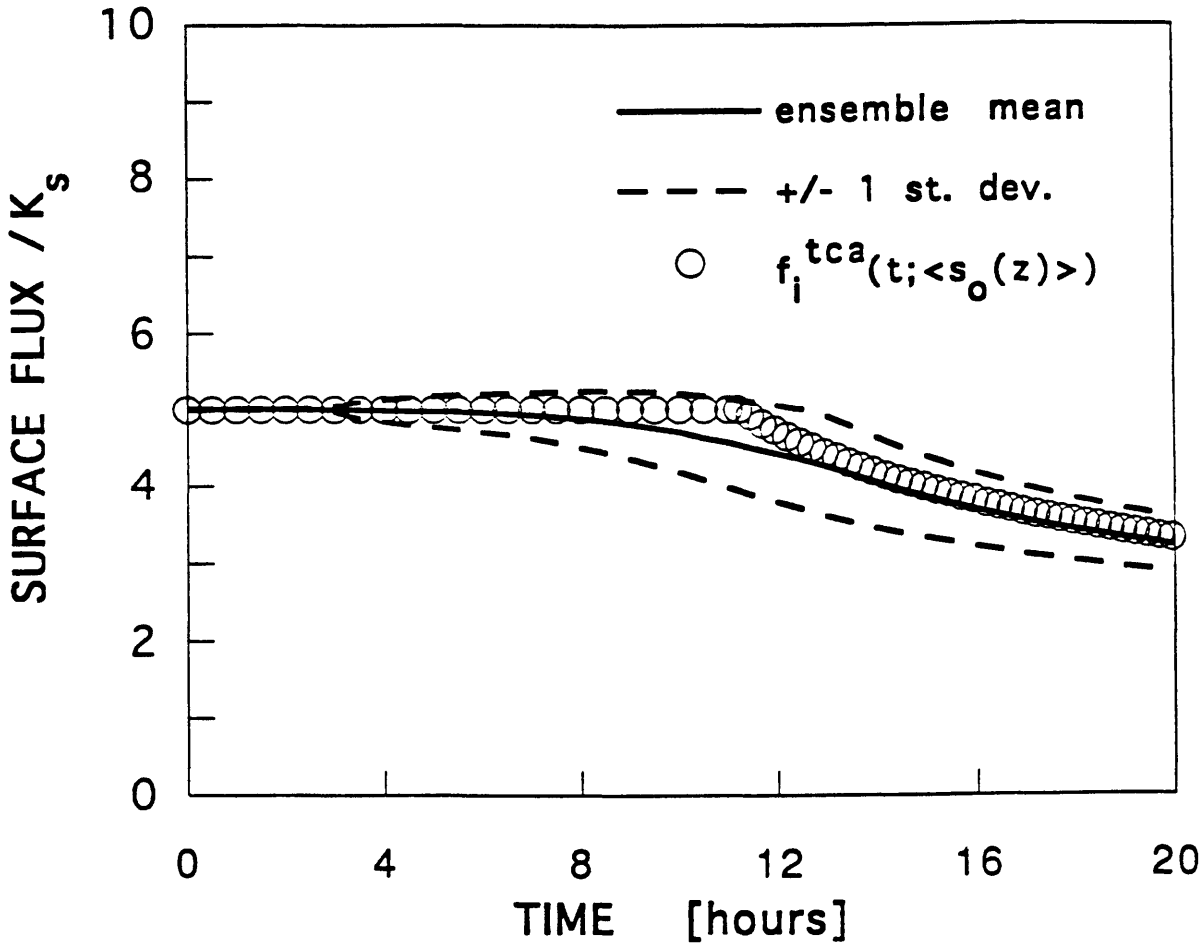

Fig. 7. Test of time compression approximation for infiltration using mean initial conditions: Deep water table case

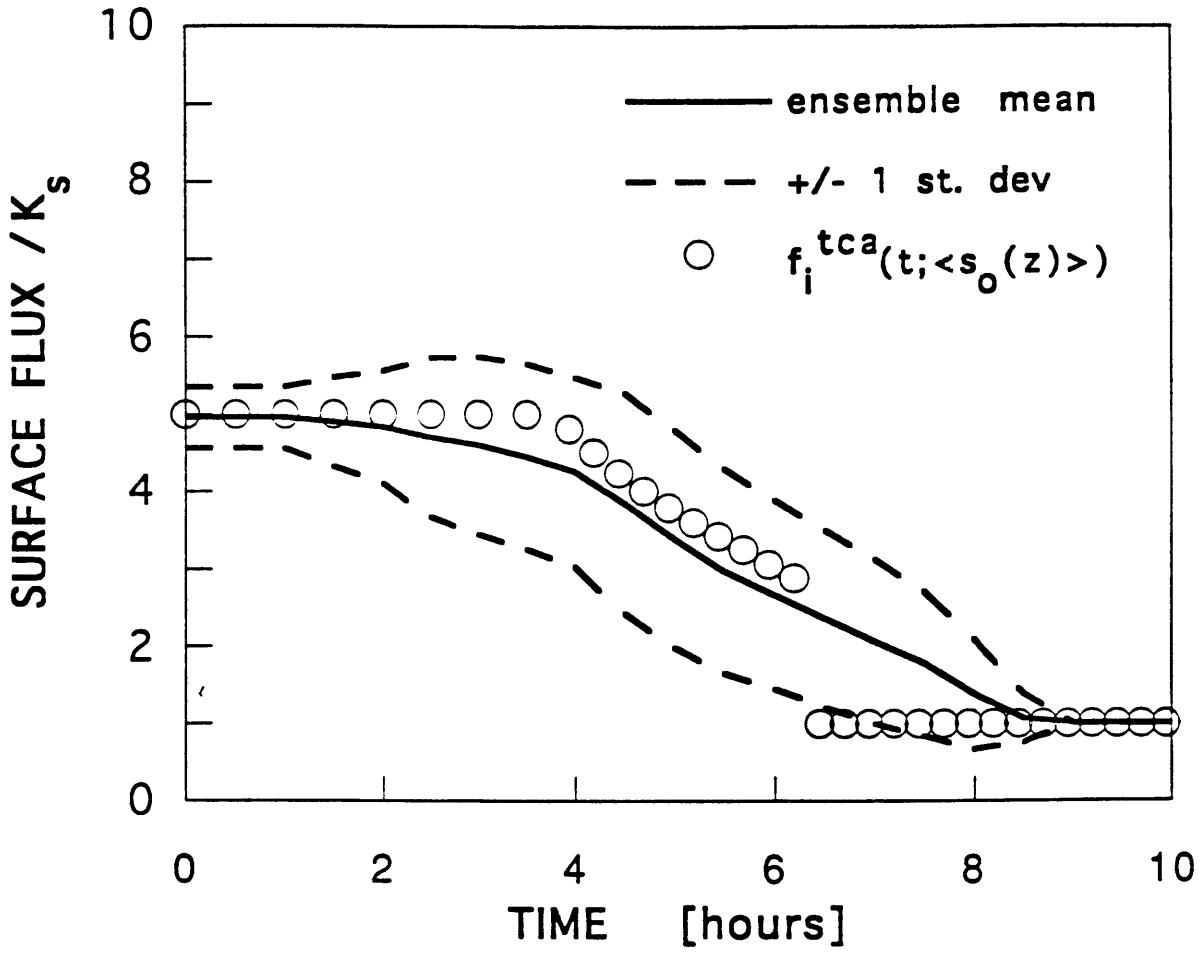

Fig. 8. Test of time compression approximation for infiltration using mean initial conditions: Shallow water table case

dynamics dominantly governed by the deep soil moisture profile. Because this deep soil moisture state is less variable from event to event than the near surface (see Figures 2 and 4), the long time flux rate is less variable. In fact, for the shallow case, there is no variability after ~ 9 hours, because the soil column is saturated and the initial condition has been completely "erased". Note that the larger variation at the intermediate times smoothes out the "kink" in the flux rate that occurs at the moment of ponding. The kink is smoothed out because each realization of the initial condition profile results in a slightly different ponding time.

To a very good approximation, the TCA appears to apply for infiltration in this "mean" sense. For example, if one knew the non-uniform mean initial moisture profile at a location in a watershed then one could use this mean profile to "initialize" the infiltration capacity curve and use the TCA expressions to estimate the infiltration for a given storm event. The infiltration capacity curve for each event may thus be generalized and a single infiltration capacity curve for a season and location may be defined. In fact, the historical success of engineering flood forecasting practices (e.g. SCS curves and regionalized empirical infiltration equations) is partly owed to this physical characteristic of the vadose zone moisture dynamics.

Any one infiltration prediction could contain significant scatter, as indicated by the standard deviation envelope. For long term mean water balance however, any given storm intensity will occur many times and thus be exposed to the full ensemble of initial condition profiles. Thus to the degree that the "mean" TCA is unbiased, the individual errors will cancel, leaving an excellent estimate of the mean infiltration for a given storm intensity.

In Figure 9 the same analysis is made under the deep water table conditions for exfiltration. For this case, one-hundred post storm moisture profiles were

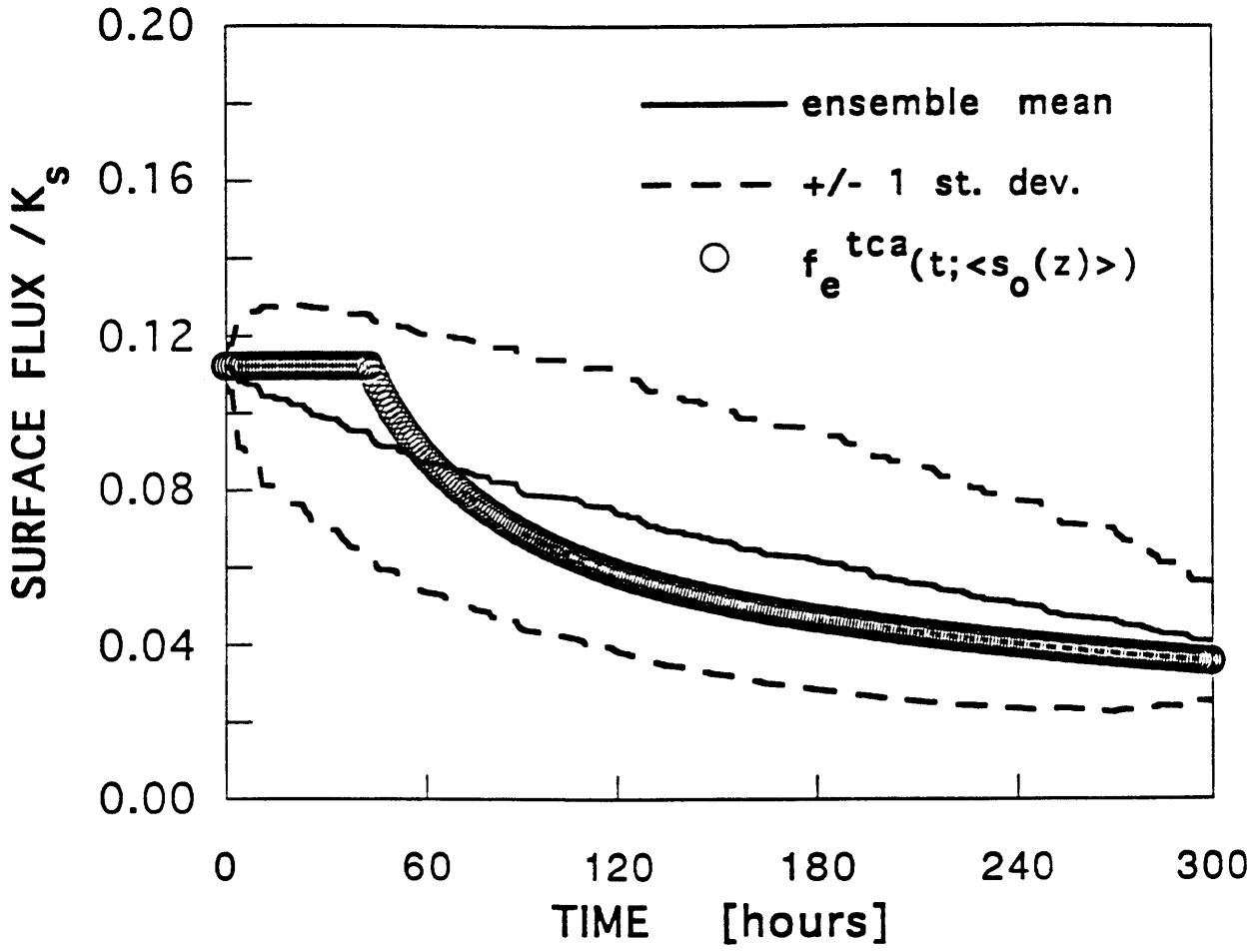

Fig. 9. Test of time compression approximation for exfiltration using mean initial conditions: Deep water table case

used as initial conditions and the potential evaporation was used as the forcing. Here the approximation is less accurate, though still reasonable for mean water balance estimation. For water balance studies, it is not the absolute deviation between the ensemble mean exfiltration curve and the "mean" TCA solution that is critical, but rather difference between the cumulative integral under the curves up to the end of the interstorm event.

As before, the variation caused by the differences in initial condition profile is largest for intermediate times. Note that the "kink" in the flux rate curve has been completely smoothed out in this case. Again, this is caused by differences in the "drying time", t_d, for each of the realizations. A similar analysis for the shallow water table case showed no soil controlled evaporation events. This is because the exfiltration capacity curve for the shallow water table is always larger than the potential evaporation forcing. This result is consistent with the water balance for the twenty year simulation (Table II), which showed actual evaporation equal to potential evaporation.

Test of the TCA under equivalent steady state initial conditions

While the results with the mean initial condition profile are interesting from a theoretical point of view, they are still partly impractical from the point of view of equilibrium water balance modelling. In general, one does not know these mean non-uniform pre-storm and pre-interstorm moisture profiles. Previously, however, we showed that the equivalent steady moisture profile formed a reasonable estimate of these mean "initial condition" profiles, with the estimate improving deeper in the soil. Summarizing the earlier results, this improvement was due to the damping out of the surface induced perturbations

with depth and the corresponding reduction in the covariance term (Eq. 12) that biased the equivalent steady estimate of the mean moisture profile.

If the infiltration and exfiltration capacity curves are not too sensitive to the near surface initial condition profile, we might then expect that the equivalent steady profile ($s_o(z; q_{st}=<q>)$), could be used as the initial condition, in place of the mean ($<s_o(z)>$). The utility of this further approximation is that the equivalent steady profile is dependent only on the mean column flow and water table depth. Methods for estimating these two parameters of the steady flow profile are discussed in the final section of this paper.

To test this further simplifying approximation, the infiltration and exfiltration capacities were simulated again, this time using the equivalent steady profiles (Figures 1 and 3) as the initial condition. The resulting "equivalent steady" TCA solutions are plotted as the circles in Figures 10, 11 and 12. Using this estimate of the pre-event initial conditions introduces some bias to the estimation of the mean surface fluxes for the deep water table infiltration and exfiltration.

For infiltration (Fig. 10), the "equivalent steady" TCA expressions underestimate the mean infiltration, particularly at intermediate times. This underestimation occurs because the equivalent steady profile overestimates the moisture content of the mean pre-storm profile (Fig. 1). For exfiltration (Fig. 11), the approximation leads to an overestimation of the mean flux, consistent with the fact that equivalent steady profile also overestimates the mean post-storm moisture profile (Fig. 1).

As mentioned previously, the cumulative rather than the instantaneous infiltration and exfiltration are the important quantities. It is thus significant that in both cases the long time behavior (which corresponds to the largest deviations from climate control) is predicted well.

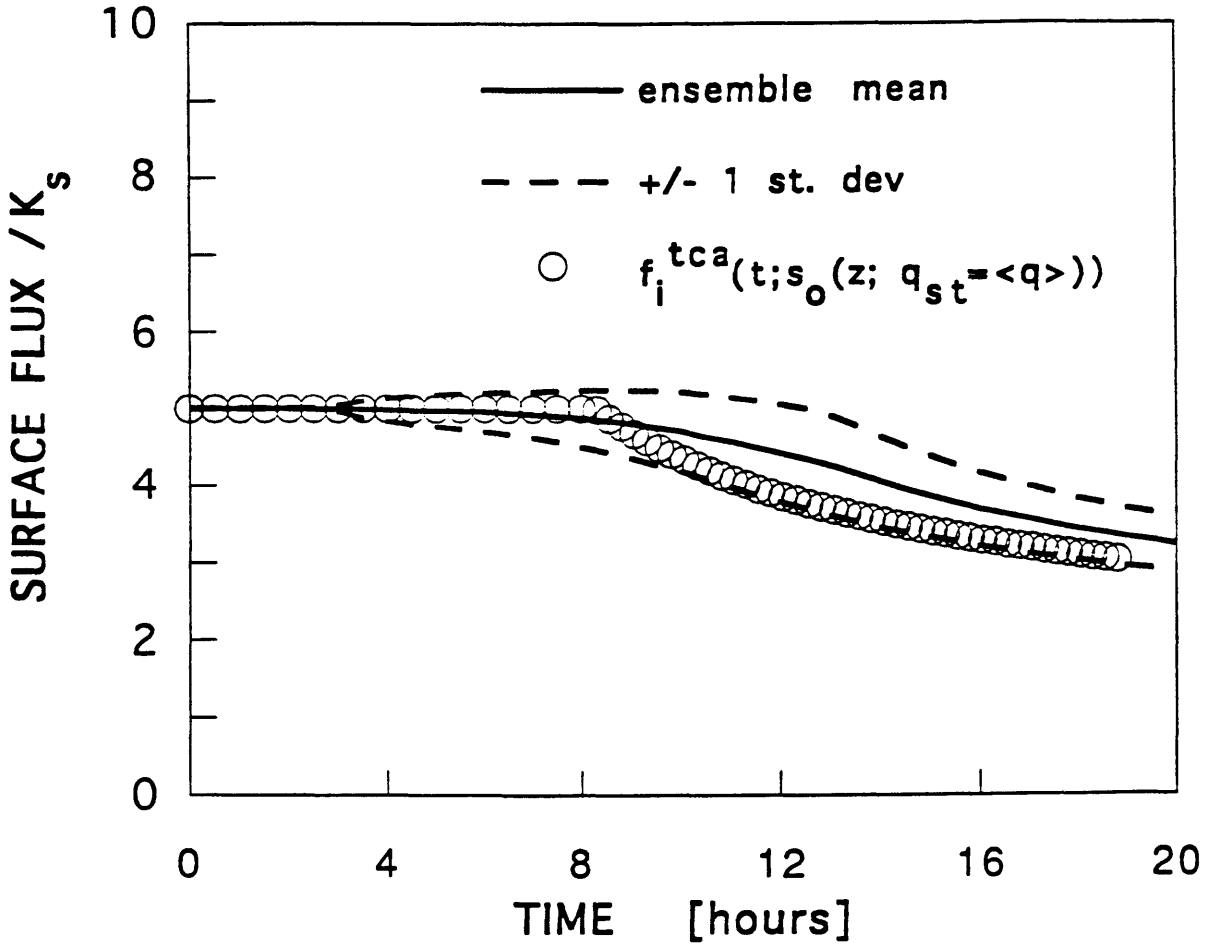

Fig. 10. Test of time compression approximation for infiltration using equivalent steady state initial conditions: Deep water table case

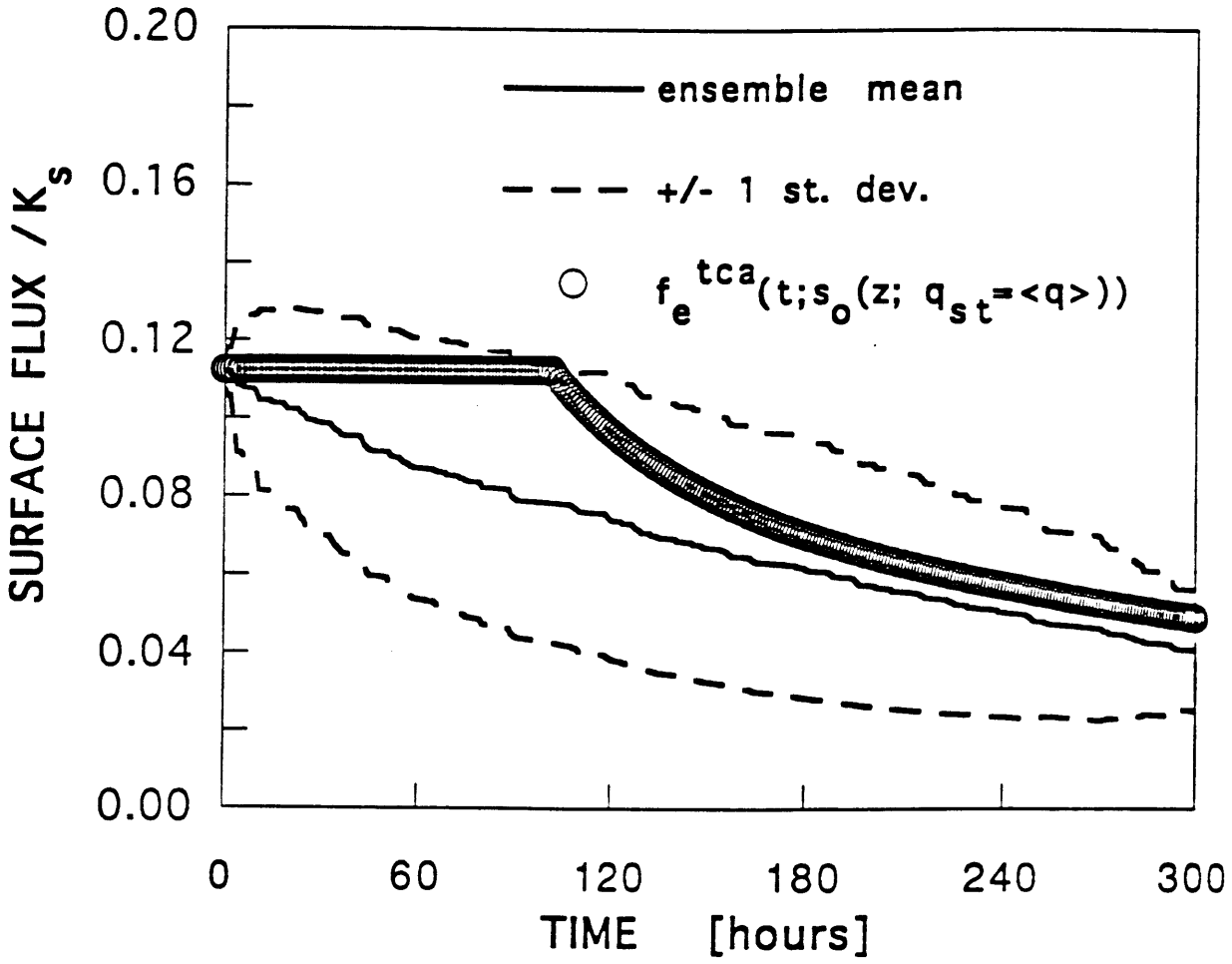

Fig. 11. Test of time compression approximation for exfiltration using equivalent steady state initial conditions: Deep water table case

Considering infiltration excess runoff, for example, the errors associated with using the equivalent steady profile to initialize flux capacities will be least for the largest runoff events, assuming (reasonably) that these events are caused by high intensity-long duration storms. The long time behavior, and thus the large soil controlled cumulative moisture exchanges, are predicted well because the role of the highly variable near surface initial condition is gradually diminished as the event continues. This is because at long durations the infiltration front penetrates deeper in the soil, leaving infiltration excess runoff generation more dependent on penetration velocities in the deeper, less variable moisture profile, where the equivalent steady profile best estimates the actual initial condition. This may be the reason why in traditional engineering approaches to initializing basins for rainfall-runoff transformation, methods that use correlations with the deep moisture state (e.g. the Antecedent Precipitation Index (A.P.I)) would give a good indication of the infiltration capacity.

For the shallow case (Fig. 12), the TCA estimation using the equivalent steady state profile as the initial condition gives slightly better estimates than using the mean intial conditions. This is contradictory to the TCA operation being linear. Apparently the overestimation of the wetness of the mean pre-storm moisture profile by the equivalent steady profile compensates for some nonlinearity in TCA operation.

In summary, the steady-state initialized TCA yields an adequate and simple means to estimate the event exchanges of moisture which occur under combinations of climate and soil controlled boundary conditions. The robustness of the approximation derives from: 1.) the fact that the TCA behaves in an approximately linear fashion with respect to initial conditions; and 2.) the fact that by the time the surface flux rate comes under soil control (e.g. t_p or t_d), the wetting (or drying) front has usually penetrated comparatively deep into the

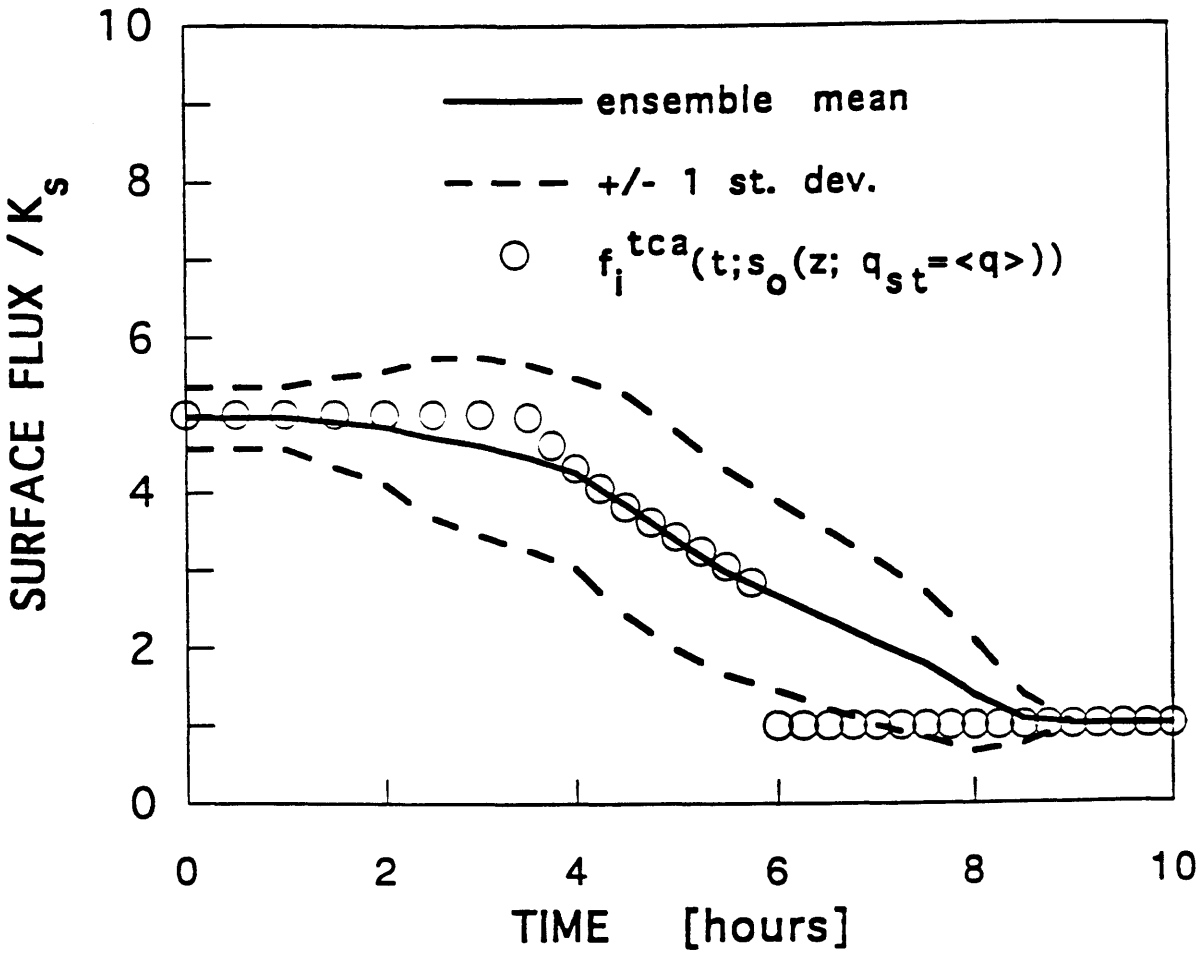

Fig. 12. Test of time compression approximation for infiltration using equivalent steady state initial conditions: Shallow water table case

soil, where the moisture state is relatively steady and thus is well estimated by the equivalent steady moisture profile.

In the above analysis, we have demonstrated these characteristics for a given soil type (clay) and a given rainstorm intensity and potential evaporation rate. In Salvucci and Entekhabi (1993), we show the results of an equilibrium water balance model whose performance is based, in a large part, on the validity of the use of the TCA and the equivalent steady-state profile. The tests are conducted for various soil textures and climate types; they provide support for the use of the TCA and for the use of the equivalent steady-state profile as an indicator of mean intial conditions under broader conditions than are demonstrated here.

Implications for event based water balance models

The major thrust of this work is on long-term equilibrium water balance modelling. Some of our results have relevance to short range, event based water balance modelling and rainfall-runoff forecasting.

A common problem in this field is specification of the initial moisture state of the watershed. The role of the initial condition is handled differently in various models, mostly depending on the type of model. Physically based, distributed models, such as TOPMODEL (Beven and Kirkby, 1979), and the model presented by Cabral et al. (1993), specify the moisture state over the spatial domain. This may be done, for example, on the basis of remotely sensed data of the near surface moisture state and some assumptions of how the profile is distributed from the surface to the water table. Likewise, one may use the position of the water table in conjunction with assumptions on the moisture profile gradient from the water table up to the surface (Sivapalan et al., 1987;

Troch et al., 1993). In each of the latter studies, the profile was assumed to be hydrostatic. This assumption will be discussed shortly.

In the absence of measurements of the moisture profile at the modelled locations in the field, the equivalent steady moisture profile should provide a reasonable, though partly biased, estimate of the initial condition for determining infiltration and exfiltration capacities. For homogeneous soils, this equivalent steady moisture profile can be found exactly for "exponential" soils (Gardner, 1958), and approximately for soils with Gardner type power law conductivities (Salvucci, 1992). For heterogeneous soils, it can be determined numerically (e.g. Warrick and Yeh, 1990). In all cases, the depth to the water table and steady flow rate (recharge or capillary rise) must be known.

The average streamflow of a given watershed and its contributing area characteristics could be used to estimate the spatial distribution of these parameters, if assumptions are made concerning the dynamics of the saturated flow domain. For example, Sivapalan et al. (1987) use the contributing area methodology of TOPMODEL and an assumption that the baseflow before a storm results from a basin-wide spatially uniform recharge, to derive the spatial distribution of the water table depth relative to the basin average water table depth. This mean depth can also be related base flow, either using the flow equations of TOPMODEL (Sivapalan et al., 1987), or assuming Boussinesq flow (Troch et al. 1993). In Salvucci and Entekhabi (1993), we present a method which relaxes the assumption of spatially uniform recharge. Instead the net flow to the saturated zone from the unsaturated zone is determined at each point by the equilibrium water balance of the overlying soil column. Basinwide water balance is then achieved by allowing the lateral redistribution of this point recharge (or capillary rise) in the saturated zone. This method incorporates the spatial effects, discussed by Penman (1951, referenced in Kuhnel et al., 1991) of "riparian" near

channel zones, where the evaporation is usually potential and runoff production significant, and "non-riparian" zones where evaporation may be soil controlled.

Assuming that one of the above methods can be used to determine the water table depth and equivalent steady flow rate, the equivalent steady profile should form a better initial condition for initializing infiltration and exfiltration capacities than the hydrostatic profile assumed by Sivapalan et al. (1987), Famiglietti and Wood (1991) and Troch et al. (1993). The degree of improvement will depend both on the depth to the water table.

For shallow water tables near channels, the steady profile is close to hydrostatic (see Figure 4). For deep water tables, however, the hydrostatic assumption may lead to serious underestimation of the wetness of the moisture profile (see Figure 1), while the equivalent steady profile would only slightly overestimate the profile's moisture content.

If used to estimate infiltration capacities from which Hortonian runoff is being calculated, the hydrostatic assumption is probably sufficient, since most of this runoff is created in the areas of high water table near the channels. For saturation excess runoff, where the generation is dependent on downslope redistribution of infiltration from uphill areas, the hydrostatic assumption could be problematic, as it would overestimate the infiltration capacity of these uphill areas. If used to estimate exfiltration capacities, as in Famiglietti and Wood (1991), it could be especially problematic since the departures of evaporation from potential will occur mostly in the drier "uphill" areas where the water table is deeper.

These effects are illustrated for the deep water table condition in Figures 13 and 14. The circles in these figures represent the TCA approximated solution using a hydrostatic initial profile in the flux capacity determination. The effect on infiltration is rather small. The impact on the exfiltration solution, however,

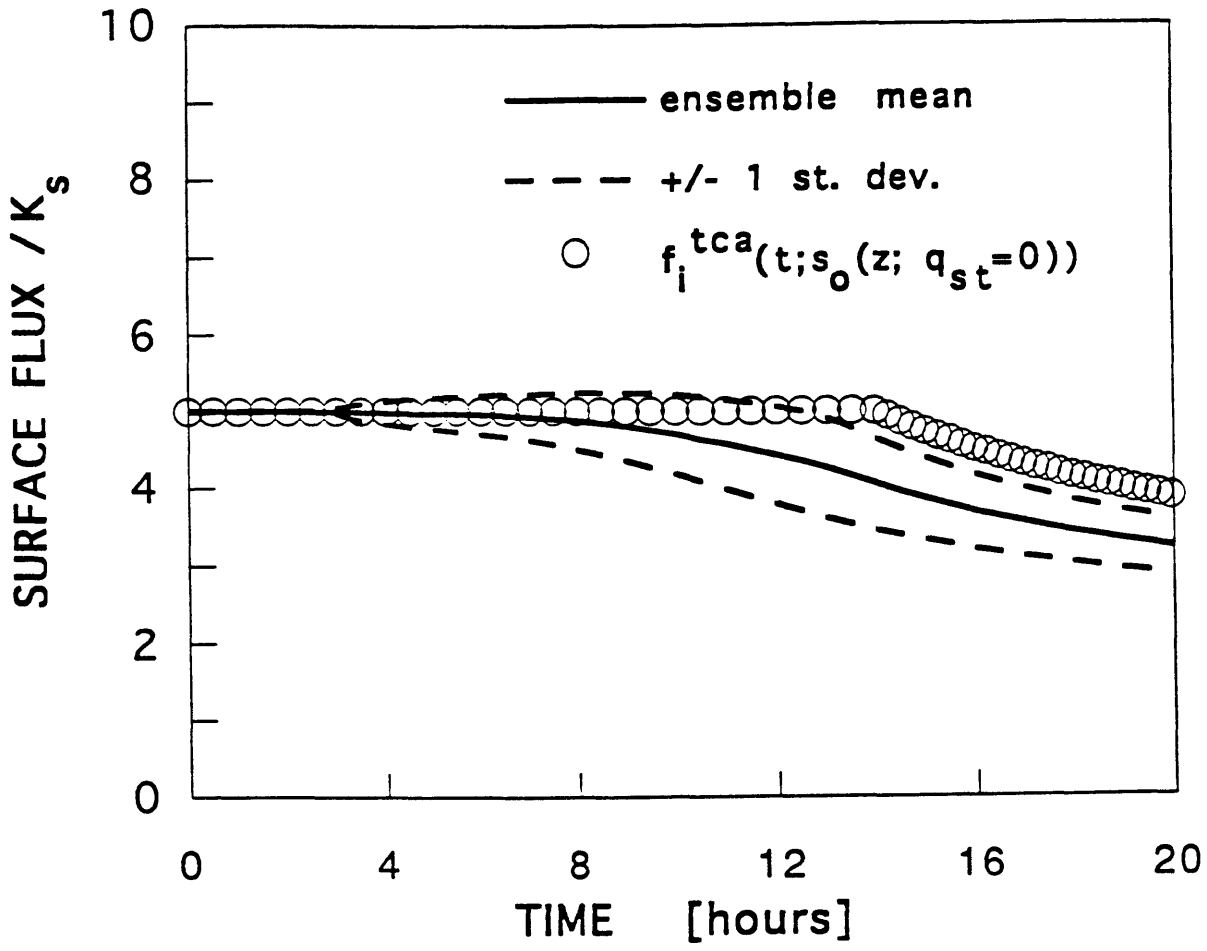

Fig. 13. Test of time compression approximation for infiltration using hydrostatic initial conditions: Deep water table case

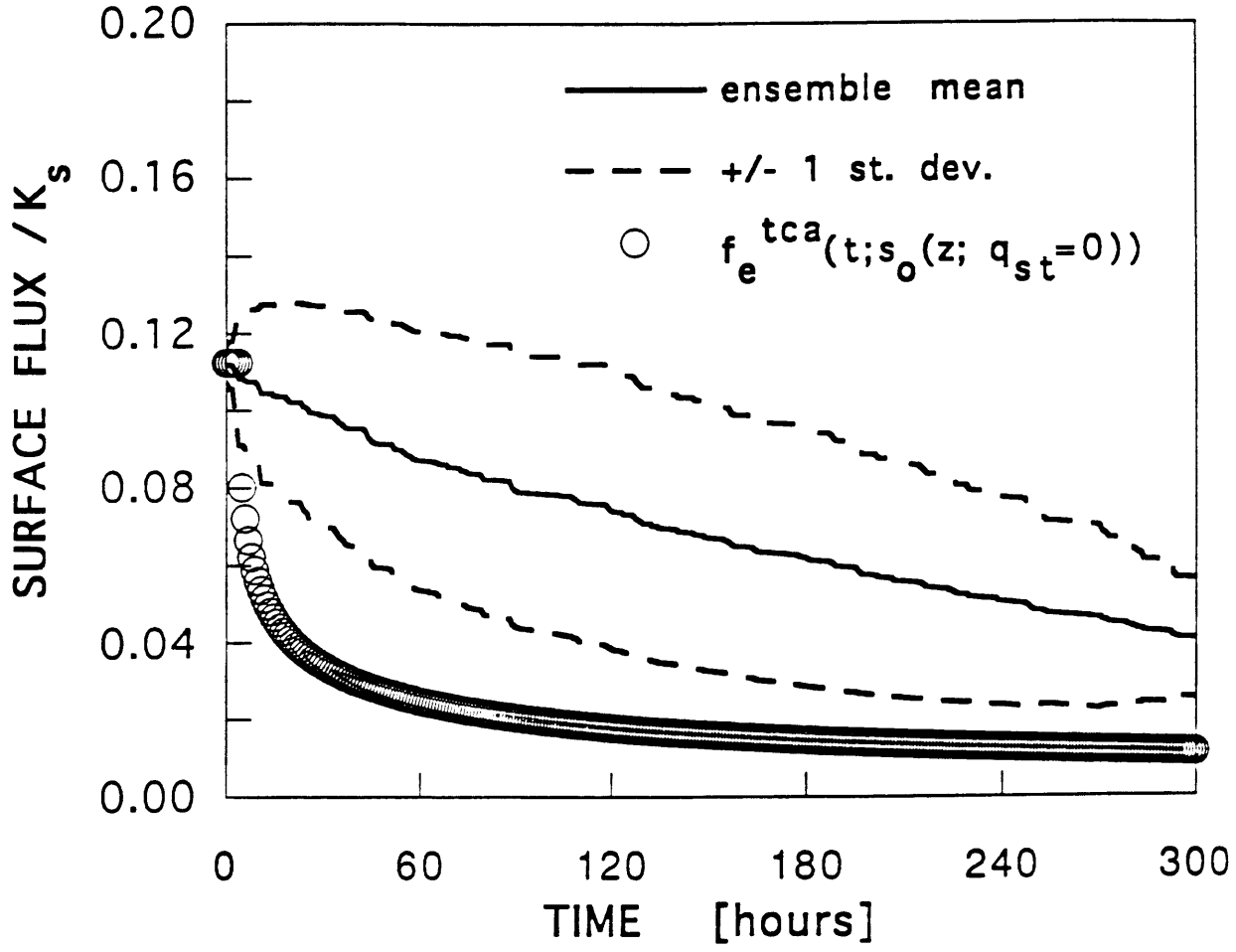

Fig. 14. Test of time compression approximation for exfiltration using hydrostatic initial conditions: Deep water table case

is significant and could cause a large underestimation of evaporation. The direction of the effect is consistent with the relative wetness of the hydrostatic profile in comparison with the mean initial condition profiles (Figure 1).

Implications for equilibrium water balance models

The role of the TCA and moisture profile characteristics in the determination of the equilibrium water balance is discussed in detail in the accompanying paper (Salvucci and Entekhabi, 1993). Here we present a short summary only.

Consider at some point in a watershed a soil column bound by the water table and the soil surface. If we assume that the significant flows in this unsaturated zone are in the vertical (i.e. all major lateral flows occur in the saturated zone), then the long term mean of the flux through the surface must equal the mean flux out of the bottom. We have shown that both of these fluxes are related to the "equivalent steady profile". The bottom flux is related directly. The top flux is related indirectly through: 1.) the relation of the infiltration and exfiltration capacities to the mean pre- and post-storm initial moisture profiles; 2.) the approximation of these mean initial condition profiles by the equivalent steady state profile; and 3.) application of these steady state initialized capacity curves to partition the surface fluxes for an ensemble of events of various duration and forcing (i and e_p) to yield the long term mean flux through the surface. For some equivalent steady profile, which can be characterized by the mean recharge (or capillary rise) and the depth to the water table, the long term continuity condition will be satisfied and the equilibrium water balance partition determined.

Note that this will be a stable equilibrium, since, for a given water table depth, larger "recharge" rates correspond to wetter equivalent steady moisture profiles, which decrease the soils infiltration capacity and increase the soil's exfiltration capacity. With less infiltration and more evaporation, the profile is dried out and the recharge diminished, bringing the system back to equilibrium.

This method of analysis also illustrates how the water table affects the surface balance. For example, the equivalent steady profile under shallow water tables conditions is more wet closer to the surface than under deep water table conditions, and thus the infiltration capacity is reduced (enhancing runoff production) and the exfiltration capacity increased (enhancing evaporation).

For deep water tables the near surface equivalent steady moisture profile becomes vertical (Fig. 4, long dashed line). Under this approximately semi-infinite condition, both the steady recharge and the surface fluxes become independent of the water table depth, and the analysis becomes identical to that given by Eagleson (1978), with the "equivalent steady profile" becoming his "equilibrium soil moisture".

In conclusion, the equilibrium water balance and the role of the water table depth in its determination can be analyzed within the framework of three relatively simple and well understood processes: time compression analysis, the steady state moisture profile, and the infiltration and exfiltration capacities found with the steady moisture profile as an initial condition. This framework requires numerical or experimental evaluation of only a few boundary value problems, i.e. the determination of the steady state solution and the two capacity curves, or possibly none, for cases where exact or approximate analytic solutions exists.

Conclusions

The equivalent steady state moisture profile, i.e. the steady moisture profile corresponding to the time average column flow, yields a sufficient estimate of the temporal mean, mean pre-storm and mean post-storm moisture profiles. It is shown that the equivalent steady and temporal mean profile are identical for "linear" soils, and that for nonlinear soils the equivalent steady profile will always overestimate the profile's moisture content.

The time compression approximation (TCA) provides an adequate description of the nonlinear, state dependent transition of surface flux from climate to soil control. It is dependent on the specification of an initial soil wetness profile. We find that the TCA is nearly linear in that the mean of surface flux histories for an ensemble of events is well reproduced by the TCA flux expression evaluated at the mean of the initial conditions of the ensemble of events. Furthermore, the mean intial condition is well approximated by the equivalent steady profile defined by the temporal mean flux (<q>) through the soil column.

APPENDIX: SOIL HYDRAULIC MODELS

The Brooks-Corey (1966) model relate the effective soil saturation (s), the capillary tension head (Ψ) and the unsaturated hydraulic conductivity (K(s)) by the following relationships:

$$s(\Psi) = \begin{cases} \left(\frac{\Psi}{\Psi_s}\right)^{-m} & \Psi \le \Psi_s \\ 1 & \Psi \ge \Psi_s \end{cases} \qquad \text{(A.1)}$$

$$K(s) = K_s \cdot s^c \qquad \text{(A.2)}$$

In the above:

$$s = \frac{\theta - \theta_r}{n_t - \theta_r} \qquad \text{(A.3)}$$

where θ is the volumetric moisture content, θ_r is the residual moisture content, and n_t is the total porosity. In addition, Ψ_s is the bubbling pressure head, which is the largest tension head at which the soil remains saturated, m is the pore size distribution index, and c is the pore disconnectedness index . On the basis of theory and experiment for a wide range of soil types, Brooks and Corey show that these two exponents can be related by:

$$c = \frac{2+3m}{m} \qquad \text{(A.4)}$$

Note that for the soil moisture diffusivity (D) defined as:

$$D(\theta) = K(\theta) \cdot \frac{d\Psi}{d\theta} \qquad \text{(A.5)}$$

the Brooks Corey relation gives the following dependence of D on s:

$$D(s) = \begin{cases} \left(\frac{-K_s \Psi_s}{mn}\right) \cdot s^{(c+1)/2} & s<1 \\ \infty & s=1 \end{cases} \qquad \text{(A.7)}$$

The exponential soil model (Gardner, 1958) relates the soil hydraulic properties by:

$$K(\Psi) = K_s \cdot e^{\alpha\Psi} \qquad \text{(A.7)}$$

$$s(\Psi) = e^{\alpha\Psi} \qquad \text{(A.8)}$$

which yields:

$$K(s) = K_S \cdot s \qquad \text{(A.9)}$$

and

$$D = \frac{K_S}{\alpha n} \qquad \text{(A.10)}$$

In the above, α is a (positive) scaling parameter with units of inverse length. While exponential relations such as A.7 and A.8 can reasonably represent $s(\Psi)$ and $K(\Psi)$ separately, it is not neccessarily the case that the length scale (α) would be the same for each relationship. This assumption is often made as it yields the above constant diffusivity and thus simplifies mathematical analysis.

REFERENCES

Abbot, M.B., J.C. Bathurst, J.A. Cunge, P.E. O'Connel, and J. Rasmussen, "An introduction to the European Hydrological System-Syteme Hydrologique Europeen, "SHE", 2, Structure of a physically-based distributed modelling system", *J. Hydrol., 87*, pp. 61-77, 1986

Beven, K.J. and M.J. Kirkby, "A physically based variable contributing area model of basin hydrology", *Hydrologic Sciences-Bulletin, 24*, 43- 69, 1979

Bras, R.L., Hydrology: an introduction to hydrologic science, Addison-Wesley Publishing Co., Inc., Reading, Massachusettes, 1990

Brooks, R.H. and A.T. Corey, "Properties of porous media affecting fluid flow", *J. Irrig. Drain. Div. Amer. Soc. Civil Eng.,IR2*, 61-88, 1966

Carslaw, H.S. and J.C. Jaeger, Conduction of Heat in Solids, Second Edition, Oxford University Press, New York, 1959

Cabral, M.C., L.Garrote, R.L. Bras, and D. Entekhabi, "A kinematic model of infiltration and runoff generation in layered and sloping soils", *Advances in Water Resources*, in press

Dagan, G. and E. Bresler, "Unsaturated flow in spatially variable fields, 1, Derivation of models for infiltration and redistribution", *Water Resour. Res., 14(6)*, 413-420 1978

Dooge, J.C.I., and Q.J. Wang, Comment on "An investigation of the relation between ponded and constant flux rainfall infiltration: by A. Poulovassilis et al.", *Water Resour. Res., 29(4)*, 1335-1337, 1993

Eagleson, P.S. "Climate soil and vegetation, 1, Introduction to water balance dynamics", *Water Resour. Res., 14(5)*, 705-712, 1978a

Eagleson, P.S. "Climate soil and vegetation, 2, The distribution of annual precipitation derived from observed storm sequences",*Water Resour. Res. ,14(5)*, 713-721, 1978b

Eagleson, P.S. "Climate soil and vegetation, 3, A simplified model of soil moisture movement in the liquid phase", *Water Resour. Res., 14(5)*, 722-730, 1978c

Eagleson, P.S. "Climate soil and vegetation, 4, The expected value of annual evapotranspiration", *Water Resour. Res., 14(5)*, 731-740, 1978d

Eagleson, P.S. "Climate soil and vegetation, 5, A derived distribution of storm surface runoff", *Water Resour. Res., 14(5)*, 7741-748, 1978e

Eagleson, P.S. "Climate soil and vegetation, 6, Dynamics of the annual water balance", *Water Resour. Res., 14(5)*, 749-764, 1978f

Eagleson, P.S. "Climate soil and vegetation, 7 A derived distribution of annual water yield", *Water Resour. Res., 14(5)*, 765-776, 1978g

Entekhabi, D., and P.S. Eagleson, "Land surface hydrology parameterization for atmospheric general circulation models including subrid scale variablilty", *J. of Climate, 2(8)*, 816-831, 1989

Entekhabi, D., I. Rodriguez-Iturbe and R.L. Bras, "Variability in large-scale water balance with land-atmosphere interactions", *J. of Climate, 5(8)*, 798-813, 1993

Famiglietti, J.S. and E.F. Wood, "Evapotranspiration and runoff form large land areas", in Land surface-Atmosphere Interaction, observations, models and analysis, E. Wood (ed.), Kluwer Academic Publishers, Norwood, Massachusettes, 179-204, 1991

Gardner, W.R., "Some steady state solutions of the unsaturated moisture flow equation with applications to evaporation form a water table", *Soil Science, 85(5)*, 228-232, 1958

Gardner, W.R., "Solutions of the flow equations for the drying of soils and other porous media", *Soil Science Society Proceedings*, 183-187, 1959

Green, W.H. and G.A. Ampt, "Studies on soils physics: I. Flow of air and water through soils", *J. Agr. Sci., 4*, 1-24, 1911

Haverkamp, R. J.-Y Parlange, J.L. Starr, G.Scmhitz and C. Fuentes, "Infiltration under ponded conditions: 3. A predictive equation based on physical paramters", *Soil Science, 149(5)*, 292-300, 1990

Hawk, K.L. and P.S. Eagleson, "Climatology of station storm rainfall in the continental United States: Parameters of the Bartlett-Lewis and poisson rectangluar pulses models", Mass. Inst. of Technol., Dept. of Civ, Eng., R.M. Parsons Lab Rept. No. 336, 1992

Hillel, D., Applications of Soil Physics, Academic Press, Inc., New York, 1980

Milly, P.C.D., "Moisture and heat transport in hysteritic, inhomogeneous porous media: A matric head-based formulation and a numerical model", *Water Resour. Res., 18(3)*, 489-498, 1982

Milly, P.C.D., "An event-based simulation model of moisture and energy fluxes at a bare soil surface", *Water Resour. Res., 22(12)*, 1680-1692, 1986

Milly, P.C.D., "Advances in modelling of water in the unsatured zone",*Transport in Porous Media, 3*, 491-514, 1988

Milly, P.C.D., and P.S. Eagleson, "Effects of spatial variability on average annual water balance", *Water Resour. Res., 23(11)*, 2135-2141, 1987

Penman, H.L. "Vegetation and hydrology", Technical Communication No.53,Commonwealth Bureau of Soils, Harpenden, 1951

Philip, J.R., "The theory of infiltration: 4. Sorptivity and algebraic infiltration equations", *Soil Science, 84*, 257-264, 1957a

Philip, J.R., "Evaporation and moisture and heat fields in the soil", *Journal of Meteorology, 14*, 354-366, 1957b

Philip, J.R., "Theory of infiltration", in Advances in Hydroscience, vol. 5, ed. Ven Te Chow, pp. 215-296 ,Academic Press, New York, 1969

Poulovassilis, A. P. Kerkides, S. Elmaloglou, and I. Argyrokastritis, "An investigation of the relation between ponded and constant flux rainfall infiltration", *Water Resour. Res., 27(7)*, 1403-1409, 1991

Protopapas, A.L. and R.L Bras, "The one-dimensional approximation for infiltration into heterogeneous soils", *Water Resour. Res., 27(6)*, 1019-1027, 1991

Reeves, M. and E.E. Miller, "Estimating infiltration for erratic rainfall",*Water Resour. Res., 11(1)*, 102-110, 1975

Salvucci, G.D., "An approximate solution to the steady flux of moisture through an unsatured homogenous soil column", submitted to *Water Resour. Res.*, 1992.

Salvucci, G.D., and D. Entekhabi, "Equilibrium water balance: 2. The Eagleson model and a quasi-analytic method for exploring the effect of the water table

on the water balance", manuscript in progress for submission to *Water Resour. Res.*

Sherman, L.K., "Comparison of F-curves derived by the method of Sharp and Holtan and of Sherman and Mayer", *Trans. Am. Gephys. Union, 24*, 465-467, 1943

Sivapalan, M., K.J. Beven, and E.F. Wood, "On hydrologic similarity, 2, A scaled model of storm runoff production", *Water Resour. Res., 23(12)*, 2266-2278, 1987

Sivapalan, M., and P.C.D. Milly, "On the relation between the time condensation approximation and the flux-concentration relation", *Journal of Hydrology,105*, 357-367, 1989

Smith, R.E. and R.H.B. Hebert, "Mathematical simulation of interdependent surface and subsurface hydrologic processes", *Water Resour. Res., 19(4)*, 987-1001, 1983

Smith, R.E., C. Corradini and F. Melone, "Modelling infiltration for multistorm runoff events", *Water Resour. Res., 29(1)*, 133-144, 1993

Troch, P.A., F.P. De Troch, and W. Brutsaert, "Effective water table depth to describe initial conditions prior to storm rainfall in humid regions", *Water Resour. Res., 29(2)*, 427-434, 1993

Warrick, A.W., and T,-C. Jim Yeh, "One dimensional, steady vertical flow in a layered soils profile", *Adv. in Water Resources, 13(4)*, 207-210, 1990

AN APPROXIMATE SOLUTION TO THE STEADY FLUX OF MOISTURE THROUGH AN UNSATURATED HOMOGENOUS SOIL

Guido Daniel Salvucci

Ralph M. Parsons Laboratory

Hydrology and Water Resource Systems

Massachusetts Institute of Technology, Cambridge Massachusetts, U.S.A.

ABSTRACT

An approximate solution is found to the differential equation governing the steady state vertical flux of moisture through an unsaturated homogenous soil characterized by power law hydraulic properties. The solution takes the form of a series which expresses the depth to the water table as a function of the capillary tension for a given rate of percolation or capillary rise. The series' first term is shown to sufficiently approximate the full solution and is inverted to obtain explicit expressions for both the capillary tension as a function of depth and flow rate and for the steady flow rate in terms of the capillary tension and depth. The latter is shown to compare favorably both to: a) existing limiting case solutions of percolation to a water table at infinite depth and capillary rise from a shallow water table to an infinitely dry surface; and b) numerical solutions of the intermediate quasi-hydrostatic condition where the magnitude and direction of flow are sensitive to both the ground surface capillary tension and the water table depth.

INTRODUCTION

Movement of moisture in the unsaturated zone of soil provides a critical coupling between the atmospheric and subsurface branches of the hydrologic cycle. The pattern in which surface soil moisture responds to the rapidly varying atmospheric boundary conditions (precipitation and evaporative demand) and the slowly varying water table depth is a critical factor in determining the location, quantity and residence time of water in the various components of the hydrologic cycle. Because of the significant latent and specific heats of water, the unsaturated zone's response also strongly affects the energy budget at the soil–atmosphere interface and thus partly determines the regional climate.

The moisture state of the near surface soil changes according to seasons and the characteristics of storms and interstorm periods. There is, however, a region at some distance from the surface (the so–called "penetration depth") below which the effects of the rapidly varying boundary conditions are damped out by the overlying diffusive medium. This leaves a quasi–steady climatic flow condition from that depth in the soil column down to the water table. At the water table boundary this steady infiltration or exfiltration is added to, or subtracted from, the regional groundwater system, which itself is coupled to the regional surface drainage network.

The unsaturated zone may therefore be conceived of as an unsteady flow region from the surface to roughly the penetration depth and a seasonally steady flow region from this point to the water table. This paper concerns itself with this seasonally steady flow region and contains the derivation of simple explicit equations which describe the moisture and flow conditions in this region. These equations illustrate the nature of the effect of water table depth on the moisture profile and the percolation or capillary rise rates. The overall effect of the water table location on the water balance can then be explored through matching of the soil moisture and

flux condition at the upper boundary of this steady region to the unsteady diffusion dominated region above it. An method for the characterization of such processes has been described by Eagleson (1978c), in which the coupling of the two systems with disparate time scales is accomplished by averaging across the storm–interstorm time scale of the upper region using derived distribution and probability theory.

In both of these regions, the equation governing the moisture state (in one dimension) is taken to be the concentration dependent convective–diffusion equation (i.e., Richard's Equation):

$$\frac{\partial \theta}{\partial t} = \frac{\partial}{\partial z}\left[D(\theta)\,\frac{\partial \theta}{\partial z}\right] + \frac{\partial K(\theta)}{\partial z} \tag{1}$$

where θ is the volumetric soil water content, z is depth (positive upward), t is time and $K(\theta)$ is hydraulic conductivity (units of L/T). $D(\theta)$, the diffusivity (units of L^2/T), is related to the conductivity through $D(\theta) = -K(\theta)\frac{d\psi(\theta)}{d\theta}$, where $\psi(\theta)$ is the capillary tension head (a positive quantity equal to the absolute value of the the capillary pressure normalized by the specific weight of water) expressed in units of length. A large base of exact and approximate analytic solutions and numerical approaches to (1) under general boundary and initial conditions have been developed (e.g., Green and Amp, 1911; Philip, 1969; Rubin and Steinhardt, 1963; Broadbridge and White, 1988; and Zimmerman and Bodvarsson, 1991).

Comparatively fewer solutions are available under the simpler (but more restrictive) steady state condition, under which Eq. (1) reduces to the Darcy equation:

$$q = +K(\theta)\left[\frac{d\psi(\theta)}{dz} - 1\right] \tag{2}$$

The complexity of analytic or numerical solution to (2) depends, as in the unsteady case, on the choice of hydraulic parameterization of $K(\theta)$ and $\psi(\theta)$ (or, equivalently, for the steady state condition, $K(\psi)$).

Philip (1957), employed numerical solutions for measured $K(\theta)$ and $\psi(\theta)$, in the more complex framework of coupled moisture and heat flux. Ripple et al. (1972) used nondimensionalization and numerical integration to present graphical solutions to (2) for a power law conductivity relationship of the form $K(\psi) = a/(\psi^n + b)$. Gardner (1958) gave an exact analytic solution for the exponential conductivity relation $K(\psi) = K_1 e^{-d\psi}$ and for the power law case for certain values of the exponent n. Anat et al. (1965) incorporated the Brooks and Corey (1966) hydraulic parameterization (a special case of the power law function) and developed an approximate solution for $n > 1$. This solution applies only to evaporation and consists of two expressions, one valid for the relatively wet section of the moisture profile, and one for the drier section. More recently Warrick (1988) showed that with the proper change of variables, the exact solution to the power law and Brooks–Corey cases can be written, for any $n > 1$, in terms of the incomplete Beta function.

In each of these works, the solution is first posed for the depth, z, as a function of the capillary tension head (ψ) and the steady flow rate (q). In addition to this form, Gardner (1958), Anat et al. (1965), Ripple et al. (1972) and Warrick (1988) inverted their solutions (and made certain approximations) to derive expressions for the dependence of evaporation on the water table depth for the limiting case boundary condition of infinite ground surface capillary tension (i.e., infinite dryness). Except for this limiting case, the solutions incorporating power law hydraulic properties are not explicitly invertible to the perhaps more useful forms $\psi(z,q)$ and $q(\psi,z)$.

In this work an approximate solution to Eq. (2) is posed for a power law conductivity function similar to that used in the above works. While the solution is

approximate, it has added utility in that it is: a) explicitly invertible from $z(\psi,q)$ to $\psi(z,q)$ and $q(z,\psi)$; b) applicable to both infiltration and capillary rise; and c) a single expression valid throughout the whole profile.

For comparison, the approximate expressions for the moisture profile and steady flow rate are compared against a trapezoidal–rule numerical integration of the governing steady flow equation (Eq. (2)). In addition the limiting case evaporation is compared with those expressions found in the literature.

PROBLEM FORMULATION

Vertical flow of moisture in the unsaturated zone is governed by Darcy's law:

$$q = -K(s) \quad \frac{d\phi(s)}{dz} \tag{3}$$

where

q	=	flow rate (cm/sec) (pos. for q in direction of z, i.e. evaporation)
K(s)	=	hydraulic conductivity (cm/sec) (a function of soil saturation)
s	=	relative soil saturation (dimensionless) equal to the volume of water divided by the pore volume available to moisture flow
ϕ	=	total energy head (cm)
z	=	vertical cartesian coordinate (positive up) (cm)

In the unsaturated zone, the energy head (ϕ) is the sum of the capillary pressure head, which is negative, and the gravitational head. With the previous definition of the capillary tension head (ψ), one obtains $\phi = z - \psi$. Eq. (3) thus becomes:

$$q = K(s)\left[\frac{d\psi(s)}{dz} - 1\right] \tag{4}$$

There are numerous models for representing the dependence of capillary tension head and hydraulic conductivity on soil saturation. The Brooks–Corey (1966) model is among the simplest in form and represents the behavior well over a large range of soil types. In this model:

$$\psi(s) = \psi_1 \, s^{-1/m} \tag{5}$$

and

$$K(s) = K_1 \; s^c \tag{6}$$

where

ψ_1 = a saturated matric potential parameter (cm)

K_1 = saturated hydraulic conductivity (cm/sec)

c = soil pore disconnectedness index (dimensionless)

m = soil pore size distribution index (dimensionless)

In addition, Brooks and Corey show (1966) that for a wide range of soil types the parameters are related by:

$$c = \frac{2 + 3m}{m} \tag{7}$$

This model yields the following dependence of K on ψ:

$$K = K_1 \left[\frac{\psi}{\psi_1}\right]^{-mc} \qquad \psi > \psi_1 \tag{8}$$

$$K = K_1 \qquad 0 < \psi \leq \psi_1 \tag{9}$$

This discontinuity in $K(\psi)$ is problematic when integrating the governing equation. We will therefore employ a power function (used, in a more general form, by Gardner (1958), Ripple et al. (1972), Anat et al. (1965), Warrick (1988) and others) of the form:

$$K(\psi) = \frac{K_1}{1 + \left[\frac{\psi}{\psi_1}\right]^n} \tag{10}$$

In the dry limit, (ψ large) this is identical to the Brooks–Corey (1966) model if we set n = mc. In the wet limit, it smooths out the discontinuity present in Brooks–Corey. Figure 1 illustrates the similarity of the two models.

Because of the wider availabilty of P(s) data (from which the parameter m can be estimated directly and the product mc indirectly through Eq. (7)), we will use Eq. (10) throughout this work but treat it as Brooks–Corey with the discontinuity smoothed out when choosing typical soil parameter values.

Incorporating Eq. (10), Eq. (4) becomes:

$$q = \frac{K_1}{1 + \left[\frac{\psi}{\psi_1}\right]^{mc}} \left[\frac{d\psi}{dz} - 1\right] \tag{11}$$

If we now normalize the flow rate (q) by K_1 (notate q′) and rearrange we obtain the following differential equation in ψ:

$$\frac{d\psi}{dz} - q' \psi_1^{-mc} \psi^{mc} - (1 + q') = 0 \tag{12}$$

subject to the water table boundary condition:

$$\psi = 0 \quad @ \quad z = 0 \tag{13}$$

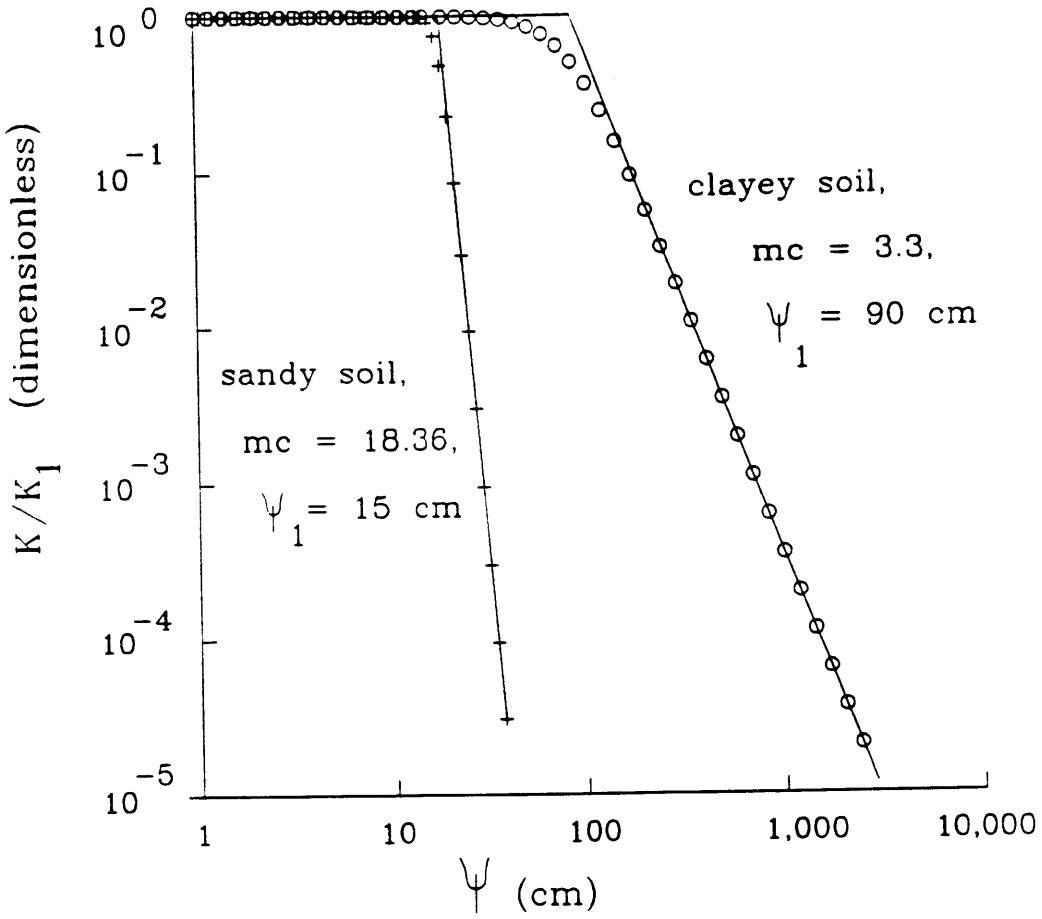

FIGURE 1: COMPARISON OF BROOKS–COREY (solid lines) AND GARDNER TYPE MODEL (pluses and circles) OF HYDRAULIC CONDUCTIVITY AS A FUNCTION OF CAPILLARY TENSION HEAD

INITIAL ANALYSIS

Analysis of the governing equation (12) reveals important limiting behaviors. First note that the normalized flow rate q' will take on values considerably less than 1 when this analysis is applied to the quasi steady region described in the introduction. In particular, when coupled to the seasonally averaged processes in the near surface soil, the maximum possible (steady state) dimensionless flow rate will be on the order of the annual potential evaporation (e.g., 50 cm) divided by the soil saturated conductivity. Likewise, the maximum possible (steady) infiltration rate will be the annual precipitation (e.g., 100 cm) divided by the soil saturated conductivity. For example, for a clay soil q' would be bounded by:

$$\frac{-100 \text{ cm/yr}}{1072 \text{ cm/yr}} \simeq -0.09 < q' < \frac{+50 \text{ cm/yr}}{1072 \text{ cm/yr}} \simeq +0.05 \qquad (14)$$

Values of K_1, ψ_1, m, c, and the approximate range of q' (calculated as they are above) are listed for three typical soils in Table 1.

With q' small in magnitude, it is clear that near the water table, where $\psi \rightarrow 0$, the profile $z(\psi)$ will be approximately linear (i.e., $d\psi/dz \simeq 1$). Also, for q' positive (evaporation) as $\psi \rightarrow \infty$ (infinite dryness), $d\psi/dz \rightarrow \infty$. For q' negative, the equation yields a limiting value for ψ of $\left[\psi_1(-q'/(1 + q'))^{-1/(mc)}\right]$, at which point $d\psi/dz = 0$. Additionally, if $q' = 0$, the hydrostatic case reveals itself as $d\psi/dz = 1$, which, subject to (13), yields $\psi = z$.

These limiting behaviors are illustrated by the numerically integrated curves in Figure 2 (adapted from Bear, 1988). Note that the two limiting asymptotes correspond to the flow solutions of $q = -K(\psi)$ for infiltration and a limiting evaporation which is not dependent on the value ψ. As mentioned in the introduction, this lack of

Table 1

Representative Values of the Brooks-Corey Soil Hydraulic Parameters and Representative Climatic Limits of the Normalized Flow Rate (q′) for Annual Precipitation of 100 cm and an Annual Evaporation of 50 cm

	K_1(cm/sec)	ψ_1(cm)	m	c	q′+	q′-
CLAY	3.4E-05	90	0.44	7.5	-0.1	0.05
SILT LOAM	3.4E-04	45	1.2	4.7	-0.01	0.005
SAND LOAM	3.4E-03	25	3.3	3.6	-0.001	0.0005

[Source: Bras, 1990]

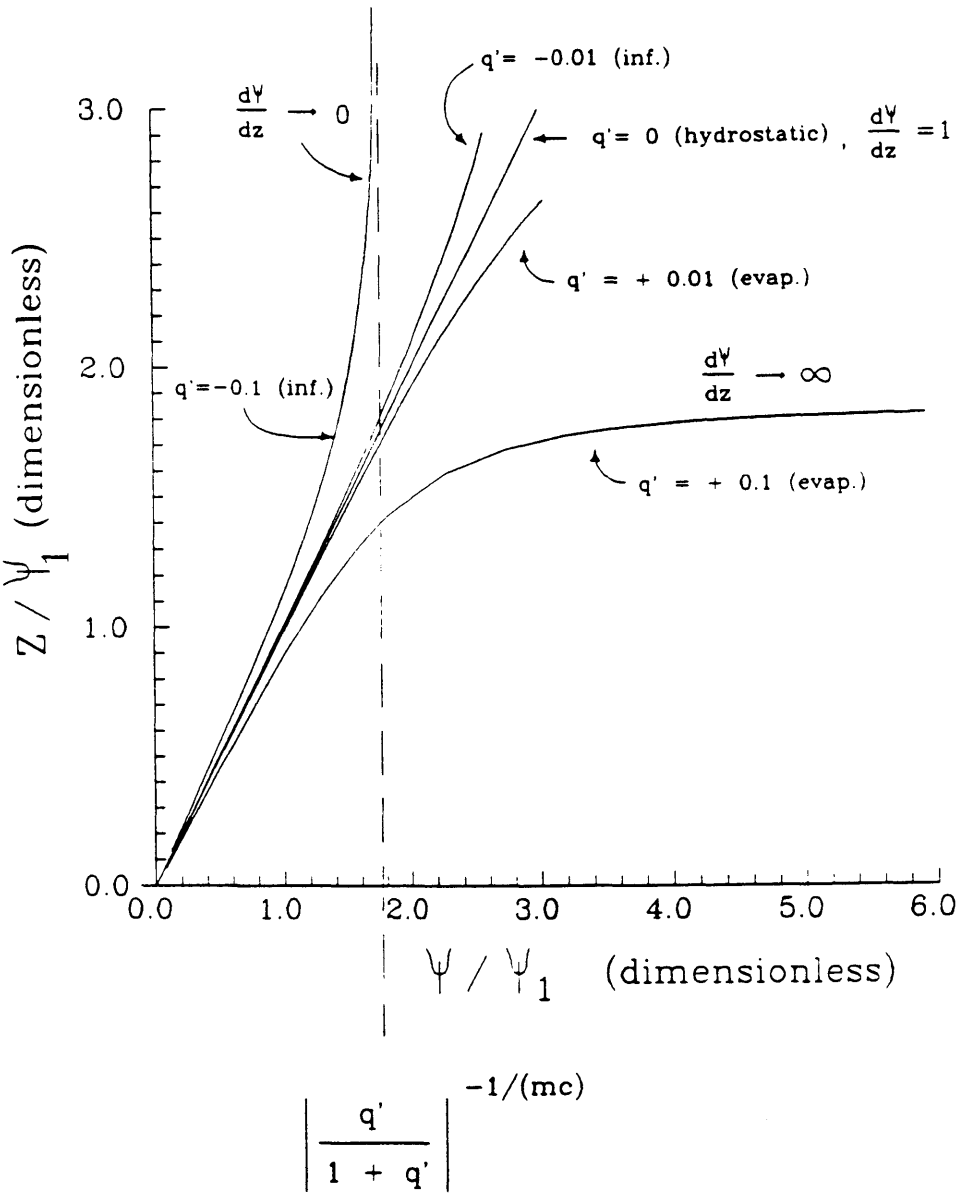

FIGURE 2: CAPILLARY TENSION HEAD PROFILES UNDER VARIOUS STEADY FLOW RATES

dependence on ψ as ψ approaches infinity has been exploited in the past to study the dependence of water table depth on maximum evaporation rates (e.g. Philip (1957), Gardner (1958), Anat et al. (1965)), Ripple et al. (1972), Warrick (1988)).

NON-DIMENSIONAL FORMULATION

The numerically integrated curves of Figure 2 reveal that most of the curvature of the solution for both infiltration and exfiltration occurs before $\psi/\psi_1 = |q'/(1 + q')|^{-1/(mc)}$ (i.e., the pressure head at which $d\psi/dz = 0$ for a given q').

Accordingly we define the nondimensional variables ψ' and z':

$$\psi' = \frac{\psi/\psi_1}{|q'/(1+q')|^{-1/(mc)}} \tag{15}$$

and

$$z' = \frac{z/\psi_1}{|q'/(1+q')|^{-1/(mc)}} \tag{16}$$

With the above, Eq. (12) becomes

$$\frac{d\psi'}{dz'} - \frac{q' \cdot |1 + q'|}{|q'|}\ \psi'^{mc} - (1+q') = 0 \tag{17}$$

For further notational simplification define:

$$f = \text{sign}(q') = \frac{q'}{|q'|} \tag{18}$$

Also note that for $q' < 1$, $|1+q'| = 1 + q'$.

The governing equation and boundary condition are now written:

$$\frac{1}{1 + q'} \cdot \frac{d\psi'}{dz'} - f \cdot \psi'^{mc} - 1 = 0 \tag{19}$$

and

$$\psi' = 0 \quad @\ z' = 0 \tag{20}$$

The solution of Eq. (19) subject to boundary condition 20 is equivalent to evaluating the definite integral:

$$z' = \frac{1}{1 + q'} \int_0^{\psi'} \frac{d\psi'}{1 + f\psi'^{mc}} \tag{21}$$

This integral is solved exactly for integer values of the exponent (mc) in Gradshteyn and Ryzhik (1980, eqs. 2.144, 2.146). The solution, however, may not be generalized since its form changes for different values of the exponent and it is only invertible for particular values of mc. Through a change of variables, Warrick (1988) expresses the integral in terms of the incomplete Beta function. While for real $n > 1$ this form is general, it too is not easily inverted.

We will thus form an approximate solution to the integral. The overriding concern in the approximations is that the final dimensional solution be: a) invertible from $z(\psi,q')$ to $\psi(z,q')$ and $q'(\psi,z)$; b) valid for both infiltration and exfiltration ($f = \pm 1$); and c) consistent with the limiting behavior for $\psi \rightarrow \infty$, $z \rightarrow \infty$, and $q' \rightarrow 0$.

APPROXIMATE SOLUTION

We will approximate the integral (21) by making a change of variables. The substitution we make should a) allow expansion of the integrand in the numerator, and b) retain the singular behavior for infiltration (f = –1) at $\psi' = 1$. Substitute

$$X = f + \psi'^{-mc} \tag{22}$$

into Eq. (21):

$$z' = \frac{-1}{mc(1 + q')} \int_{\infty}^{X} \frac{(X - f)^{-1/(mc)}}{X} dX \tag{23}$$

Upon expanding the binomial in (23), term by term integration becomes possible. Note that for evaporation f = +1, and thus X > 1 for all ψ' (viz. Eq. (22)). Expanding the binomial around X will thus lead to a converging approximation.

For infiltration, however, f = –1 and thus X will be greater than one for the range $0 < \psi' < 2^{-1/(mc)}$, while for $2^{-1/(mc)} < \psi' < 1$, X will be less than one (viz. Eq. (22)). Therefore, if we expand the numerator of the integrand in (23) around X, the approximation will be divergent near $\psi' = 1$. In this region, the first term of an expansion around X will yield $X^{-1-1/(mc)}$, while expanding around f (which we should do for X < 1), will yield X^{-1}. When mc is large, the difference is negligible and the limiting behaviors are identical. We may thus consider the first term (and only the first term) of the expansion around X to be an approximation of the first term of the expansion around f.

For the purpose of obtaining a single expression applicable over the entire range of pressures and valid for both infiltration and exfiltration, we will choose to expand around X, even though the expansion is not strictly correct over part of the domain of interest. Note, however, that higher order terms should not be kept in the infiltration case because the expansion does indeed diverge over part of the range of ψ', while higher order terms may be retained for the convergent exfiltration case. This point will be illustrated and discussed further.

Expanding the numerator of the integrand with the binomial expansion around X, dividing by the denominator X, and integrating term by term yields:

$$z' = \frac{+1}{mc(1+q')} \sum_{k=0}^{\infty} \left[\frac{(-f)^k}{+k+\frac{1}{mc}}\right] \left[\begin{matrix}-1 \\ mc \\ k\end{matrix}\right] X^{-k-\frac{1}{mc}} \Bigg]_{\infty}^{x} \tag{24}$$

Substituting back with Eqs. (15), (16), (18) and (22) and evaluating for the boundary conditions, one obtains for the first three terms:

$$\begin{aligned}\frac{z}{\psi_1} \simeq{}& \frac{1}{1+q'} \cdot \left\{\left[\frac{q'}{1+q'}\right] + (\psi/\psi_1)^{-mc}\right\}^{-1/(mc)} \\ &+ \frac{q'}{(1+q')^2} \cdot \frac{1}{mc(mc+1)} \cdot \left\{\frac{q'}{1+q'} + (\psi/\psi_1)^{-mc}\right\}^{-1-1/(mc)} \\ &+ \frac{q'^2}{(1+q')^3} \cdot \frac{(mc+1)}{2(mc)^2(2\,mc+1)} \cdot \left\{\frac{q'}{1+q'} + (\psi/\psi_1)^{-mc}\right\}^{-2-1/(mc)}\end{aligned} \tag{25}$$

Note that in the above the n'th term is multiplied by $q'^{(n-1)}$, revealing that the magnitude of the higher order terms falls rapidly.

In Figures 3 through 5, the depth–tension head profile as calculated using Eq. (25) with 1, 2, and 3 terms is compared with the numerical solution for the typical soils (mc ranges from 3.3 to 11.88) and flow conditions ($-.1 < q' < .05$) listed in Table 1. In all three soil types, the approximation under evaporation conditions (positive q') improves as more terms are included. The improvement is most obvious in the dry limit asymptote (i.e., the horizontal part of the profile) and it depends upon soil type. For the clayey, lower valued mc soils (Figures 3 and 4), the higher order terms yield more improvement than for the sandy, higher valued mc soil (Figure 5). Also note that while including higher order terms under infiltration conditions improves (slightly) the approximation for small ψ, it deteriorates the approximation for ψ near its limiting value (i.e., the vertical part of the profile). As mentioned previously, this is due to the divergence of the expansion (for $q' < 0$, such that $f = -1$) in the latter range. This behavior is clearly illustrated in all three figures (3–5) where the 2–term approximation diverges to negative infinity and the 3–term approximation overestimates the depth z.

In summary, only the first term of (25) can be kept under conditions of infiltration, and (to a reasonable approximation) only the first term is necessary to be kept under conditions of exfiltration. In general, therefore, the first term of (25) provides a simple and reasonable approximate solution to the steady–state tension head profile under both conditions.

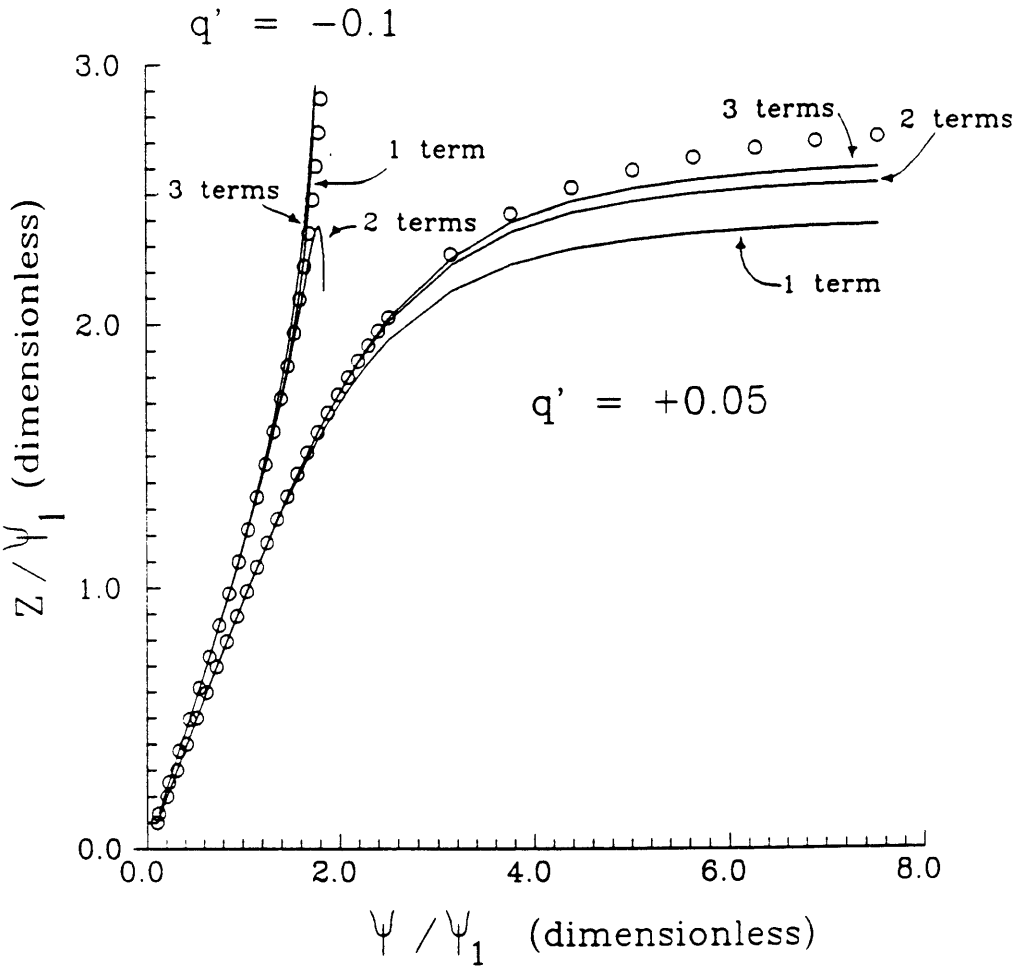

FIGURE 3: COMPARISON OF APPROXIMATE CAPILLARY TENSION HEAD PROFILES (solid lines) AND NUMERICAL SOLUTION (circles) FOR CLAY (mc = 3.3)

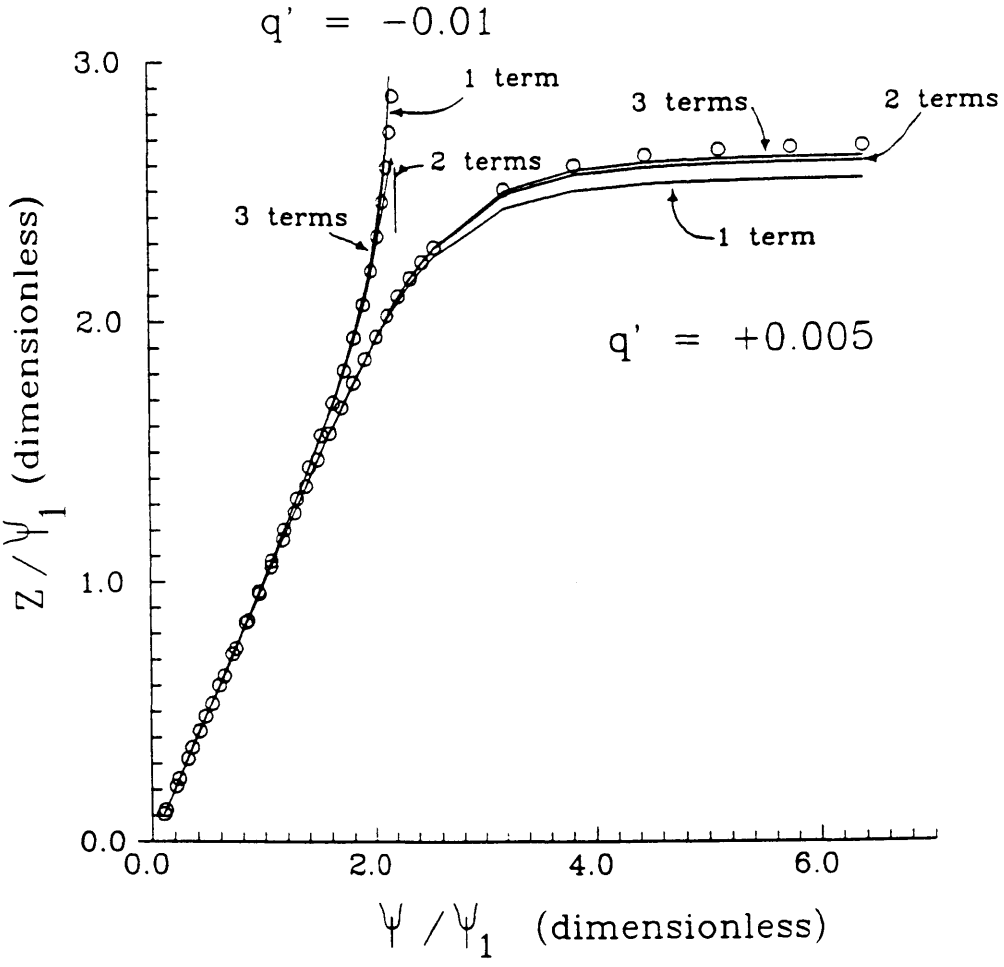

FIGURE 4: COMPARISON OF APPROXIMATE CAPILLARY TENSION HEAD PROFILES (solid lines) AND NUMERICAL SOLUTION (circles) FOR SILT-LOAM (mc = 5.64)

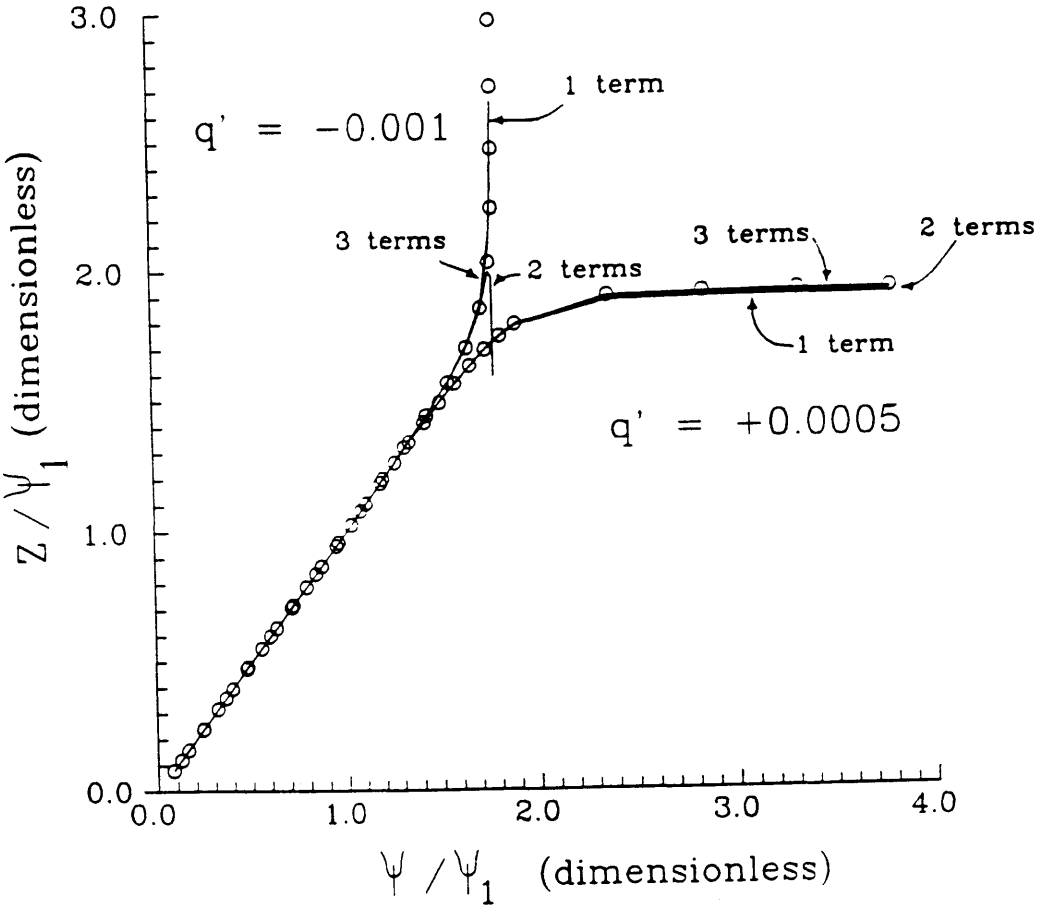

FIGURE 5: COMPARISON OF APPROXIMATE CAPILLARY TENSION HEAD PROFILES (solid lines) AND NUMERICAL SOLUTION (circles) FOR SAND-LOAM (mc = 11.88)

INVERSION

Retaining only the first term of Eq. (25) one obtains:

$$z/\psi_1 \approx \frac{1}{1 + q'} \cdot \left\{ \frac{q'}{1 + q'} + \left[\frac{\psi}{\psi_1} \right]^{-mc} \right\}^{-1/mc} \tag{26}$$

This is easily inverted to obtain $\psi(z,q')$:

$$\psi/\psi_1 \approx \left\{ \frac{-\ q'}{1 + q'} + (1 + q')^{-mc}\ (z/\psi_1)^{-mc} \right\}^{-1/(mc)} \tag{27}$$

The overriding goal of this work was to obtain an expression for $q'(\psi,z)$. An approximate implicit equation can be found by again keeping only the first term of Eq. (23) and rearranging it to obtain:

$$q' \approx \frac{\left[\frac{z}{\psi_1} \right]^{-mc}}{1 + \left[\frac{\psi}{\psi_1} \right]^{-mc}} \cdot (1 + q')^{1-mc} - \frac{\left[\frac{\psi}{\psi_1} \right]^{-mc}}{1 + \left[\frac{\psi}{\psi_1} \right]^{-mc}} \tag{28}$$

Note in Table 1 that as mc increases, the approximate applicable limit of q' decreases rapidly (i.e. high values of mc correspond to sandy soils whose conductivity is also high such that the climatic steady state limit of q' becomes very small). We may thus expand $(1 + q')^{1-mc}$ without losing very much accuracy. This allows us to solve for q' explicitly:

$$q' = \frac{\left[\left[\frac{z}{\psi_1} \right]^{-mc} - \left[\frac{\psi}{\psi_1} \right]^{-mc} \right]}{1 + \left[\frac{\psi}{\psi_1} \right]^{-mc} - (mc - 1) \left[\frac{z}{\psi_1} \right]^{-mc}} \tag{29}$$

Note that this solution exhibits the following limiting behavior:

a) $\psi = z$ . . . . . .

$$q' = 0 \qquad \text{(hydrostatic)} \tag{30}$$

b) $z \longrightarrow \infty$ . . . . . .

$$q' = \frac{-\left[\frac{\psi}{\psi_1}\right]^{-mc}}{1 + \left[\frac{\psi}{\psi_1}\right]^{-mc}} = \frac{-K(\psi)}{K_1} \qquad \text{(percolation to infinitely deep water table)} \tag{31}$$

c) $\psi \longrightarrow \infty$ . . . . . .

$$q' = \frac{\left[\frac{z}{\psi_1}\right]^{-mc}}{1 - (mc-1)\left[\frac{z}{\psi_1}\right]^{-mc}} \qquad \text{(evaporation from water table to infinitely dry surface)} \tag{32}$$

Also note that, to the first approximation, Eq. (29), represents the sum of the two limiting cases (percolation to and evaporation from water table). That the solution to the full boundary value problem could be approximated by the sum of the two limiting cases was assumed by Eagleson in his water balance model (1978c).

These limiting behaviors, and the general performance of the approximation, are illustrated in Figures 6 through 8. In these figures Eq. (29) and the numerical solution are plotted as $q'(z/\psi_1)$ for given values of ψ/ψ_1 for the three soil types. The fit appears to be a satisfactory approximation over the whole range. The best fit is for small q' (where $\psi/\psi_1 \approx z/\psi_1$) and the weakest fits occur in the dry limit of

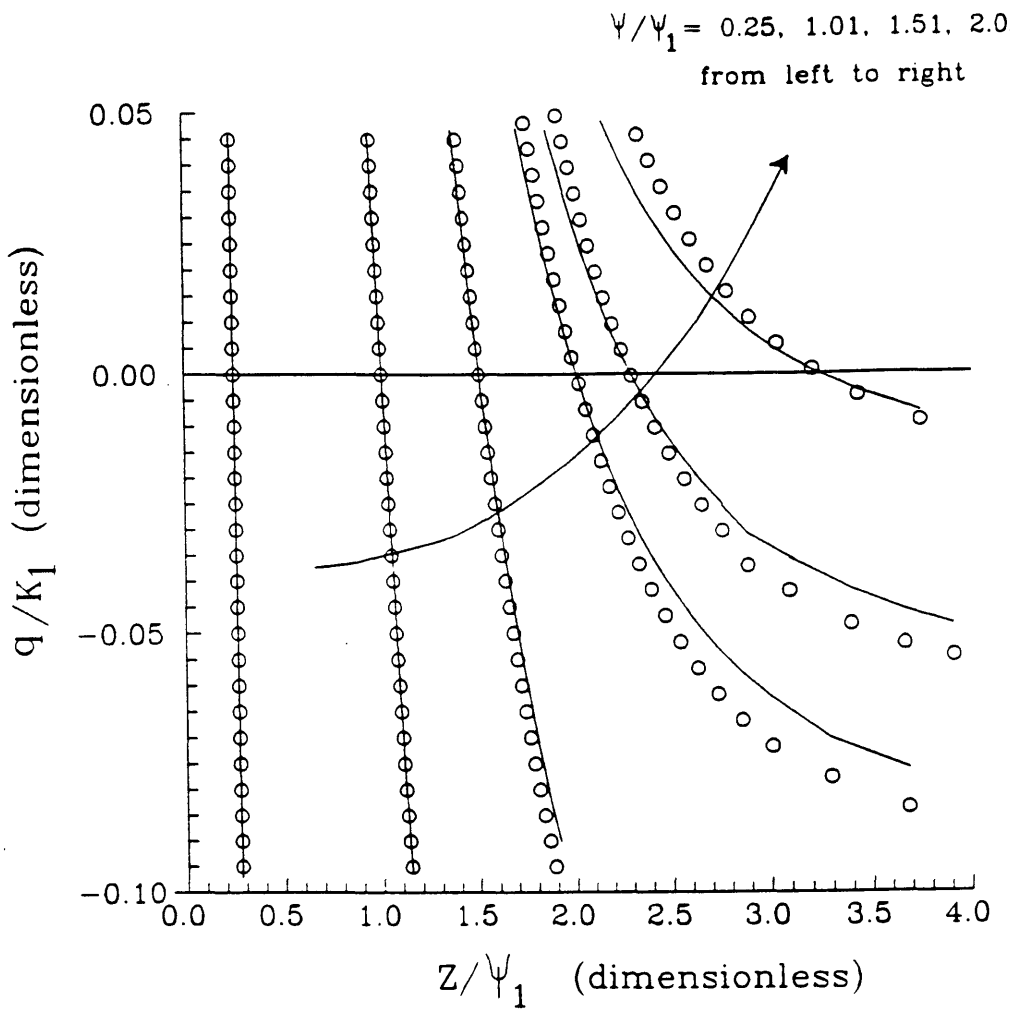

FIGURE 6: COMPARISON OF APPROXIMATE STEADY STATE FLOW RATE (solid lines) AND NUMERICAL SOLUTION (circles) FOR CLAY (mc = 3.3)

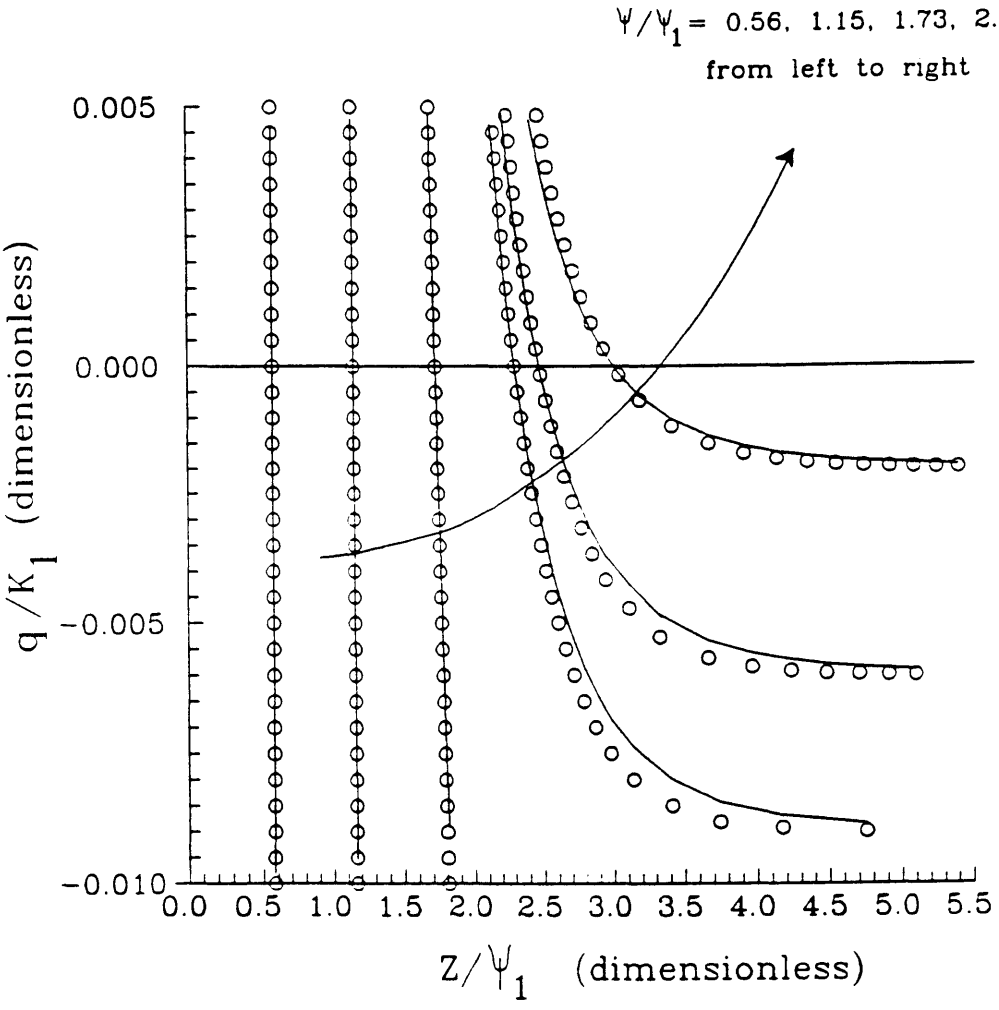

FIGURE 7: COMPARISON OF APPROXIMATE STEADY STATE FLOW RATE (solid lines) AND NUMERICAL SOLUTION (circles) FOR SILT-LOAM (mc = 5.64)

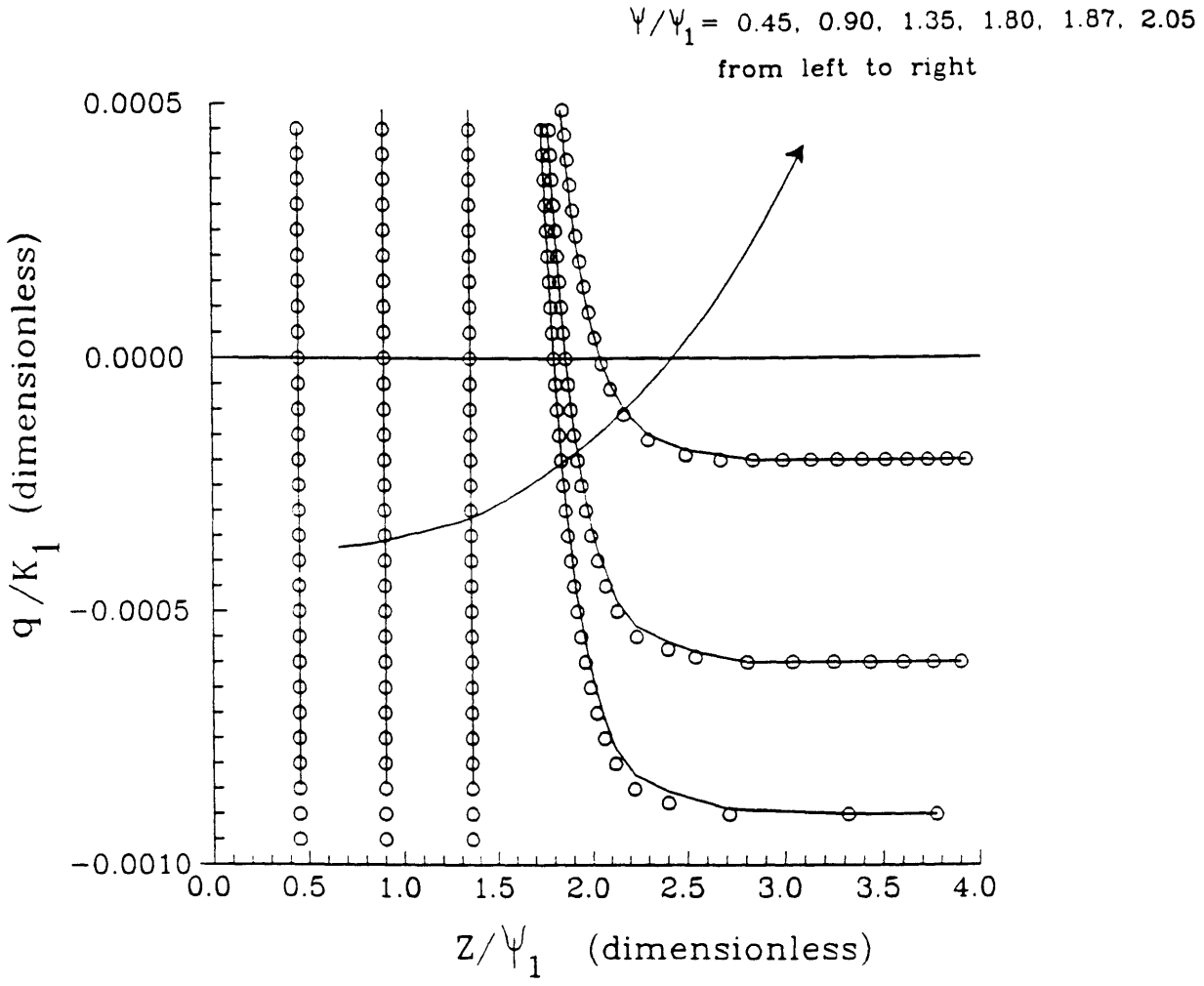

FIGURE 8: COMPARISON OF APPROXIMATE STEADY STATE FLOW RATE (solid lines) AND NUMERICAL SOLUTION (circles) FOR SAND-LOAM (mc = 11.88)

evaporation, where Eq. (29) underestimates q', and in the range just before the infiltration asymptote (where the dependence of q' on z vanishes). The error in the evaporation limit arises from neglecting the higher order terms of the $z(\psi,q')$ series (Eq. (25)). The error in the infiltration limit arises from the incorrect expansion of the integrand of (23) as ψ' approaches one. As was the case for the moisture profiles, the error is less for larger values of mc, or sandy soils (Figure 8) than for the clayey ones (Figures 6 and 7). In the evaporation case this is because the neglected higher order terms of (25) are multiplied by factors of order $(1/(mc))^2$. In the infiltration case it is because the incorrect expansion of the integrand of (23) gave $X^{-1-(1/mc)}$ while expanding about f would give X^{-1}. As mc gets larger, the difference becomes negligible.

Eq. (29) and Figures 6 through 8 also illustrate that the influence of the water table depth depends on how dry the surface is and the soil type. Capillary rise from a "shallow" water table and percolation to a "deep" water table are often treated as separate phenomena. This formulation (Eq. (29)) explicitly demonstrates that "shallow" and "deep" are relative to surface moisture state and yields a rational method to discriminate between the two conditions.

The limits taken in Eqs. (30) and (31) illustrate that the approximate solution (29) becomes exact for the hydrostatic limit and for the infinitely deep water table limit. The evaporation limit (32), however, is not exact.

For this limiting case evaporation rate, the exact solution is found by setting the surface boundary condition to $\psi = \infty$. For this case, Eq. (22) gives $X = f = 1$. Evaluating (23) with this limit (Gradsthteyn and Ryzhik (1980), 3.192(4)), redimensioning with (15) and (16), and rearranging the result yields:

$$q' = (1 + q')^{(1-mc)} \left[\frac{\pi}{mc \sin\left[\frac{\pi}{mc}\right]} \right]^{mc} \left[\frac{z}{\psi_1} \right]^{-mc} \tag{33}$$

This exact implicit solution is identical to that found by Ripple et al. (1972) and Warrick (1988) if the hydraulic conductivity parameterization employed in those references is made equivalent to (10). For example, the form used by Warrick, $K(\psi) = a/(\psi^n + b)$ will be equivalent to (10) if we set $n = mc$, $a = K_1 \cdot \psi_1^{mc}$ and $b = \psi_1^{mc}$.

Figures 9 through 11 compare this exact implicit solution with Eq. (29) (evaluated for $\psi = \infty$) for the three typical soils and some typical flow rates (Table 1). The improvement over the approximation, due to the exclusion of higher order terms in the derivation of (29), is most significant for the clayey soils (Figures 9 and 10) and less for the sandy soil (Figure 11). Eq. (29) can also be compared with the following approximate, but explicit, limiting case evaporation formulae derived by:

Anat et al. (1965):

$$q' = \left[1 + \frac{1.886}{1 + (mc)^2}\right]^{mc} \left[\frac{z}{\psi_1}\right]^{-mc} \tag{34}$$

Eagleson (1978) based upon the work of Gardner (1958):

$$q' = \left[1 + \frac{3}{2\left[mc - 1\right]}\right] \left[\frac{z}{\psi_1}\right]^{-mc} \tag{35}$$

Ripple et al. (1972) and Warrick (1988):

$$q' = \left[\frac{\pi}{mc \sin\left[\frac{\pi}{mc}\right]}\right]^{mc} \left[\frac{z}{\psi_1}\right]^{-mc} \tag{36}$$

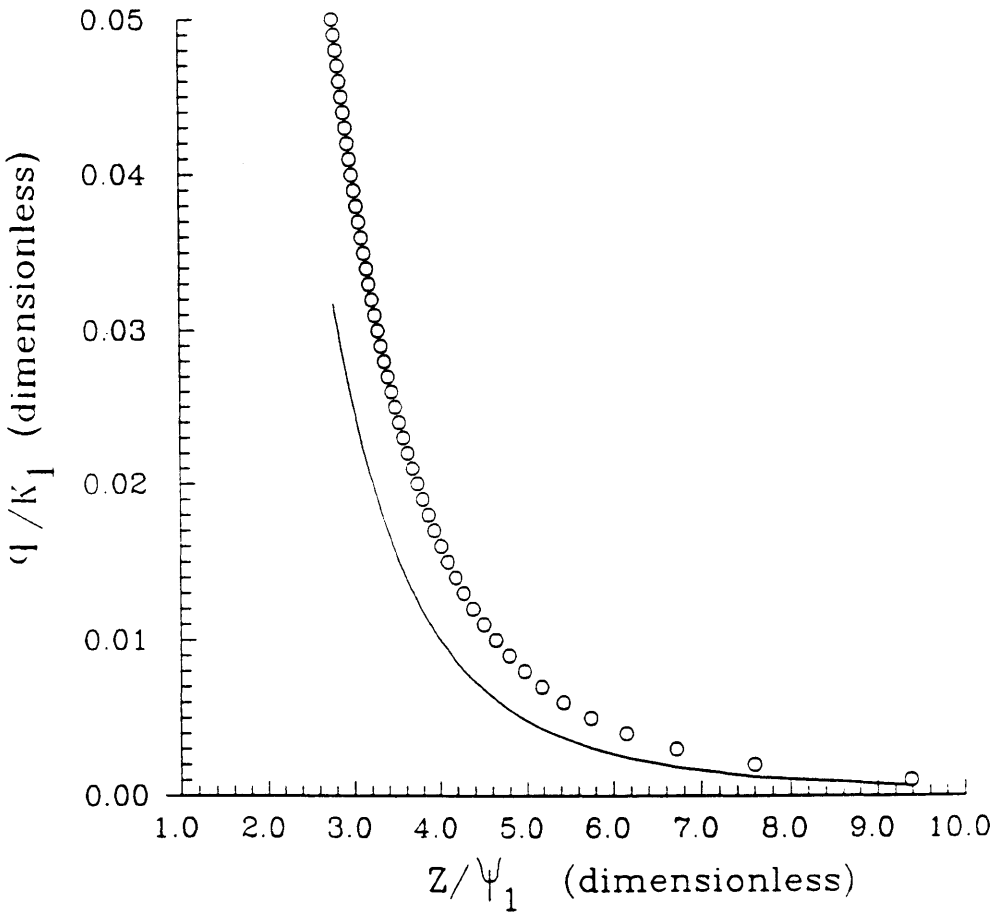

FIGURE 9: COMPARISON OF APPROXIMATE LIMITING CASE EVAPORATION RATE (solid line) AND EXACT SOLUTION (circles) FOR CLAY (MC = 3.3)

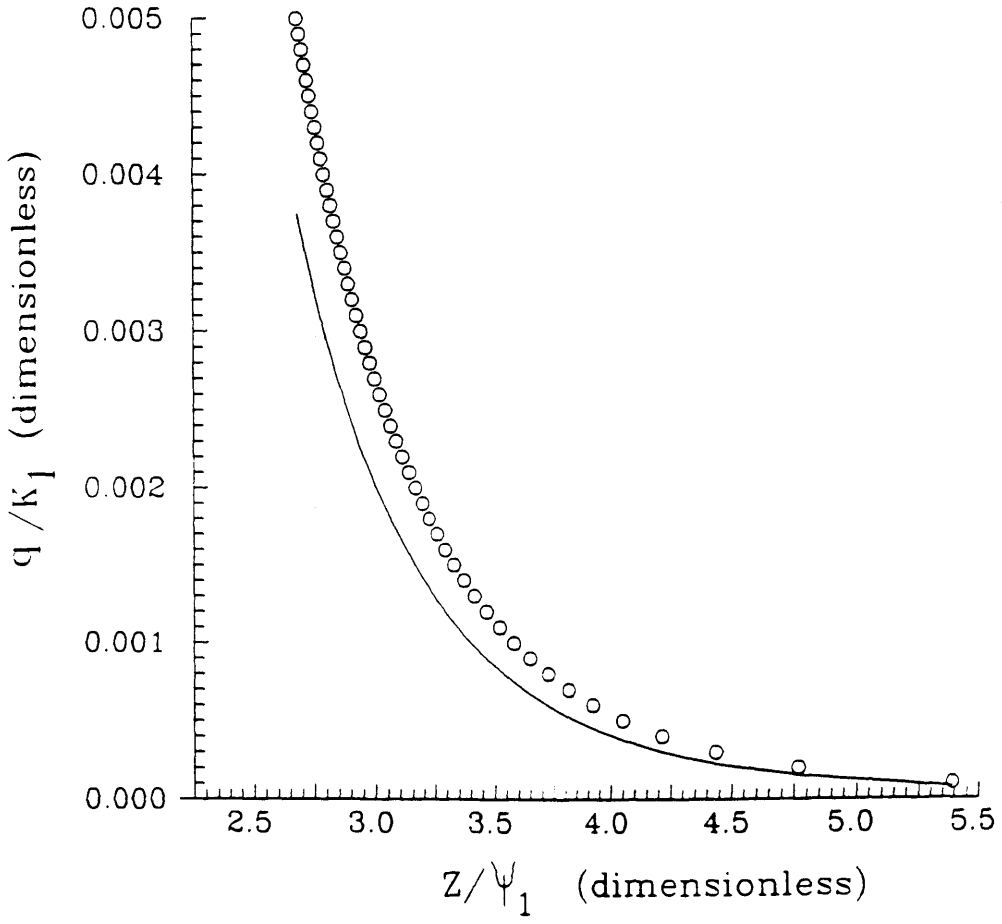

FIGURE 10: COMPARISON OF APPROXIMATE LIMITING CASE EVAPORATION RATE (solid line) AND EXACT SOLUTION (circles) FOR SILT-LOAM (mc = 5.64)

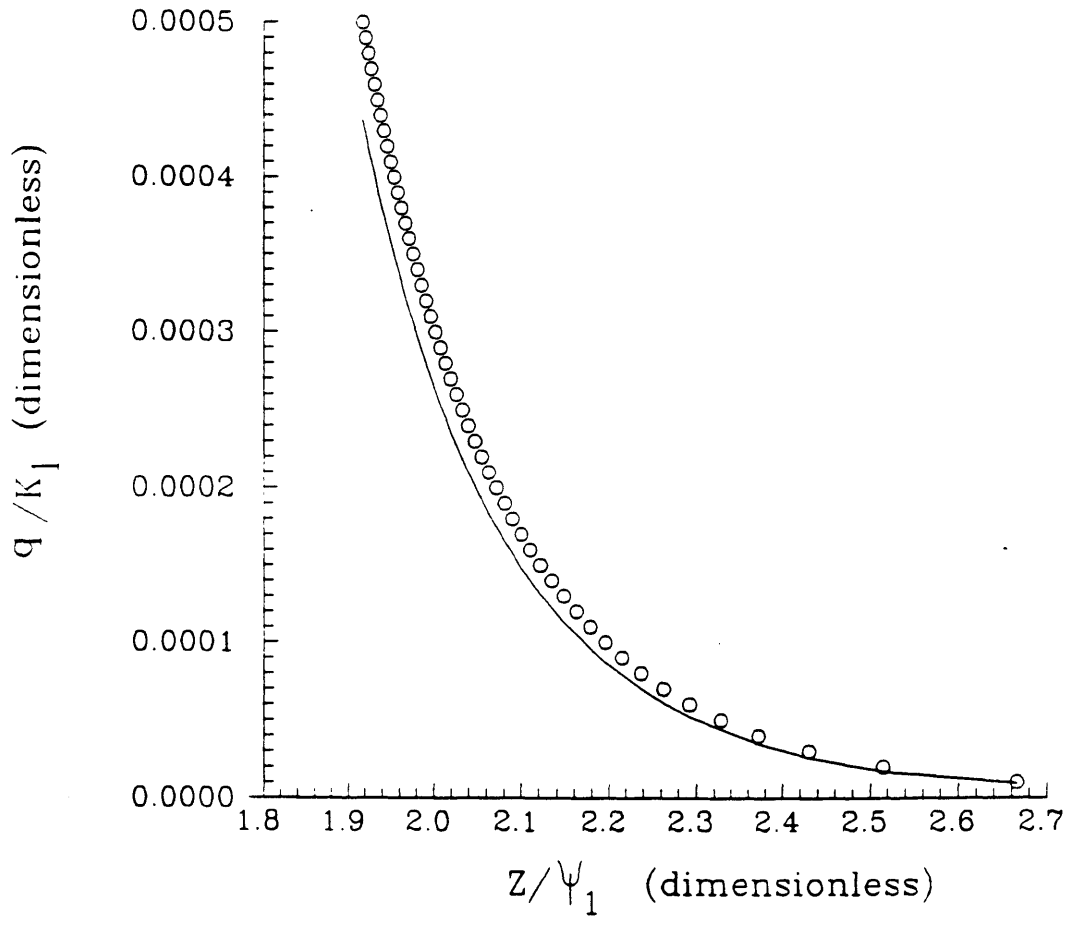

FIGURE 11: COMPARISON OF APPROXIMATE LIMITING CASE EVAPORATION RATE (solid line) AND EXACT SOLUTION (circles) FOR SAND–LOAM (mc = 11.88)

Each of these expressions is some function of mc multiplied by $(z/\psi_1)^{-mc}$. While the different references give different functional forms for the dependency on the product mc, they all give similar results. For comparison, Table 2 gives an example of the relative error of each expression by comparing them for the flow rate and soil type combinations listed in Table 1. The relative error is calculated (with the exact implicit expression (Eq. 33) as a reference case) using:

$$\text{Rel. Error} = \left| \frac{q_{approx.} - q_{exact}}{q_{exact}} \right| \tag{37}$$

Overall, Eq. (29) performs worse, in this limiting case, than the existing solutions.

Table 2

Comparison of Relative Error of Limiting Evaporation Formulae

	mc	q′	Gardner/ Eagleson	Anat	Ripple Warrick	This Work (Eq. 29)
CLAY	3.3	0.05	.11	.09	.12	.28
SILT LOAM	5.64	0.005	.01	.04	.02	.22
SAND LOAM	11.8	0.0005	.00	.02	.01	.12

CONCLUSION

An analytically simple approximation has been found for a) the steady state flow rate in an unsaturated soil in terms of the capillary tension (or soil saturation) at some distance from the water table and b) the steady state moisture profile ($z(\psi,q')$ or $\psi(z,q')$). The approximations work well over a wide range of soil types. They correctly capture the limiting behaviors of percolation to an infinitely deep water table and evaporation to an infinitely dry surface. In addition, the new solution is valid for the quasi–hydrostatic cases when the magnitude and direction of flow are sensitive to both the water table depth and the ground surface capillary tension.

NOTATION

a,b	Parameters of Gardner type power law hydraulic parameterization
c	Soil pore disconnectedness index of the Brooks–Corey hydraulic parameterization, dimensionless
d	Parameter of Gardner type exponential hydraulic parameterization
f	Variable equal to positive one for evaporation of negative one for infiltration
j,k	Counting indices of summation series, dimensionless
m	Soil pore size distribution index of the Brooks–Corey hydraulic parameterization, dimensionless
n	exponent of Gardner type power law
q	Steady state flow rate, positive for evaporation, negative for infiltration, cm/sec
s	Relative soil saturation, equal to the volume of water divided by the pore volume available to moisture flow, dimensionless
t	Time, sec
z	Vertical cartesian coordinate (positive up), cm
$D(\theta)$	Soil moisture diffusivity, cm^2/sec
$K(\theta)$	Hydraulic conductivity, cm/sec
K_1	Saturated hydraulic conductivity, cm/sec
θ	Volumetric soil water content, dimensionless

ϕ Total energy head, cm

ψ_θ Capillary tension head: a positive quantity equal to the absolute value of the (negative) capillary pressure normalized by the specific weight of water; also referred to as matric potential, cm

ψ_1 A saturated matric potential parameter of the Brooks–Corey hydraulic parameterization, cm

$[\,]'$ Scaled, nondimensional $[\,]$

REFERENCES

Anat, A., H. R. Duke, and A. T. Corey, Steady upward flow from water table, Hydrology Papers, CSU 7, 1965.

Bear, J., Dynamics of Fluids in Porous Media, Dover Publications, Inc., Mineola, 1988.

Bras, R. L., Hydrology: an introduction to hydrologic science, p. 352, Addison–Wesley Publishing Company, Inc., Reading, Massachusetts, 1990.

Broadbridge, P. and I. White, Constant rate rainfall infiltration: A versatile nonlinear model, 1, analytic solution, Water Resour. Res., 24, 145–154, 1988.

Brooks, R. H., Properties of porous media affecting fluid flow, J. Irrig. Drain. Div. Am. Soc. Civ. Eng., 92(IR2), 61–88, 1966.

Eagleson, P. S., Climate, soil and vegetation, Water Resour. Res., 14, 705–776, 1978a–g.

Gardner, W. R., Some steady state solutions of the unsaturated moisture flow equation with application to evaporation from a water table, Soil Science, 85(5), 1958

Gradshteyn, I. S. and I. M. Ryzhik, Table of Integrals, Series, and Products, Academic Press, Inc., New York, 1980.

Green, W. H. and G. A. Ampt, Studies in soil physics, 1, the flow of air and water through soils, J. Agric. Sci., 4, 1–24, 1911.

Philip, J. R., Evaporation, moisture and heat fields in the soil, Journal of Meteorology, 14(1), 354–366, 1957.

Philip, J. R., Theory of infiltration, Adv. Hydrosci., 215–296, 1969.

Ripple, C. D., J. Rubin and T. E. A. van Hylckama, Estimating steady state evaporation rates from bare soils under conditions of high water table, Geological Survey Water Supply Paper 2019A, 1972.

Rubin, J. and R. Steinhardt, Soil–water relations during rain infiltration, 1, Theory, Soil Sci. Soc. Am. J., 27, 246–251, 1963.

Warrick, A. W., Additional solutions for steady–state evaporation from a shallow water table, Soil Sci., 146, 63–66, 1988.

Zimmerman, R. W. and G. S. Bodvarsson, A simple approximate solution for horizontal infiltration in a Brooks–Corey Medium, Transport in Porous Media, 6, 195–205, 1991.